Mimochrome, a metalloporphyrin-based catalytic swiss-knife†

Linda Leone,[1,§] Marco Chino,[1,§] Flavia Nastri,[1] Ornella Maglio,[1,2] Vincenzo Pavone[1] and Angela Lombardi[1,*]

[1] Department of Chemical Sciences, University of Napoli "Federico II", Via Cintia, 80126 Napoli (Italy)

[2] IBB - National Research Council, Via Mezzocannone 16, 80134 Napoli (Italy)

[§] **These authors contributed equally to the work.**

*** Address for correspondence:**
Prof. Dr. Angela Lombardi, Department of Chemical Sciences, University of Napoli "Federico II", Via Cintia, 80126 Napoli. Tel: +39 081 674418; e-mail: alombard@unina.it

RUNNING TITLE: ***Mimochrome: a catalytic swiss-knife***

† In memory of Maurizio Bruschi, our esteemed Colleague at the University of Milano-Bicocca.

Synopsis (50-250 words)

Over the years, Mimochromes, a class of miniaturized porphyrin-based metalloproteins, have proven to be reliable but still versatile scaffolds. After two decades from their birth, we retrospectively review our work in Mimochrome design and engineering, which allowed us developing functional models. They act as electron-transfer miniproteins or more elaborate artificial metalloenzymes, endowed with peroxidase, peroxygenase and hydrogenase activities. Mimochromes represent simple yet functional synthetic models that respond to metal ion replacement and non-covalent modulation of the environment, similarly to natural heme-proteins. More recently, we have demonstrated that the most active analogue retains its functionality when immobilized on nanomaterials and surfaces, thus affording bioconjugates, useful in sensing and catalysis. This review also briefly summarizes the most important contributions to heme-protein design from leading groups in the field.

Key words: Artificial Metalloenzymes; Bioinorganic chemistry; Catalysis; Heme-protein models; Peptide scaffold; Protein design

List of abbreviations: ABTS, 2,2'-azino-bis(3-ethylbenzothiazoline-6-sulfonic acid); Aib, 2-aminoisobutyric acid; AuNPs, gold nanoparticles; Bfr, bacterioferritin; C*c*P, cytochrome *c* peroxidase; Cyt, cytochrome; C-I, compound I; C-II, compound II; Hb, hemoglobin; HCO, heme copper oxidase; HER, hydrogen evolution reaction; HRP, horseradish peroxidase; IDO, indoleamine-2,3-dioxygenase; ITO, indium-titanium oxide; Mb, myoglobin; MC, Mimochrome; MP, microperoxidase; NADH, nicotinamide adenine dinucleotide; NiR, nitrite reductase; NMH, N-methyl-histidine; NOR, nitric oxide reductase; PCET, proton coupled electron transfer; PDB, protein data bank; P450, cytochrome P450; QM/MM, quantum mechanics/molecular mechanics; RMD, restrained molecular dynamics; SHE, standard hydrogen electrode; SiR, sulfite reductase; TDO, tryptophan-2,3-dioxygenase; TFE, 2,2,2-trifluoroethanol; TON, total turnover number

1 INTRODUCTION

The idea that a chemist is able to master and forge ~~the~~ natural matter and the elements according to his/her desire is still permeating our collective imagination. In this respect, we are now aware that Nature, through evolution, is the real master. Nature has been able to bow kinetics and thermodynamics to make life not only possible, but also predominant on Earth. We have learned, through the study of an exponentially growing number of biological structures, that this was accomplished by ~~striving~~ selecting only few elements [1–4], few molecules [5–7], and even few repetitive folding motifs [8–13]. This last aspect may appear surprising at a first glance, but it actually sounds pretty comfortable to chemists, who learned over centuries that the synthesis and/or functionalization of analogues from a starting framework moiety is advantageous and generally affordable, both in terms of synthetic pathway and economic cost. This process is generally adopted in chemistry to modulate physico-chemical properties (e.g. solubility, polarity, absorption/emission spectrum) and/or functional features (e.g. acidity/basicity, nucleo/electrophilicity, redox potential, kinetics). However, in this endeavour, Nature outclasses chemists by putting in the pot, together with an amazing synthetic proficiency, a vast number of subtle interactions belonging to the realm of the "soft matter". Altogether these skills enabled the wonderful biodiversity of the ecosystem. Nonetheless, we, as chemists, still share with Nature the same language, thus ~~being a deontological imperative~~ it is our duty to learn its recipes and make use of the worth of knowledge delivered for us.

Porphyrin cofactors, and more in general tetrapyrroles, may be considered as the archetypal example, demonstrating that properly built interactions, following the lesson from Nature, may be terrifically fruitful for chemists. Such cofactors are ubiquitous and are essential in several crucial functions, from oxygen transport, redox reactions and electron transfer to photosynthesis [14]. Probably, they have been selected by evolution for their inertness (either in terms of metal complex stability or undesired ring-opening/oxidation) [15–19], which may appear unexpected, given the wide range of functions they perform. Nonetheless, this spectacular task is possible thanks to the fine-tuning of the cofactor chemical properties, which are perfectly balanced [20]. Such modulation acts at least at three different levels: (i) nature of the metal center (or its lack); (ii) modification of the molecular scaffold (e.g. identity and number of substituents, saturation); (iii) covalent and non-covalent interactions from the surrounding host (Figure 1).

Figure 1. Should be here

Wise "design" at these three levels affects the cofactor coordination sphere (complex geometry, metal/ligand affinity, complex stability) [21], and its conformational freedom (in/out-of-plane distortions) [22,23], electrochemistry (electron transfer, substrate activation) [24], and photochemistry (energy of the ground and excited states) [25].

Inspired by Nature, the scientific community has devoted many efforts to replicate this wise design, with the aim of developing artificial molecules endowed with functions.

The present review is mainly intended to give an exhaustive retrospective to the strategy we selected for developing artificial heme-proteins. Starting from a brief discussion of the strategy adopted by Nature to modulate metalloporphyrin reactivity, the most important contributions of other research groups to the field of heme-protein inspired design and engineering will be described. Finally, the results we obtained to date on the Mimochrome (MC) family of miniaturized heme-proteins will be reported in detail.

1.1 Tetrapyrrole cofactor modulation in natural proteins

Metal ion type and tetrapyrrole ring chemical composition are generally coupled in natural proteins, in order to specify different functions. Tetrapyrrole macrocycles may be found as light harvesting moieties, with or without a bound Mg ion, as in chlorophylls and bacteriochlorophylls [26]. The matrix effect, exerted by the protein environment, is determinant for their biological activity. First, the interactions within the surrounding protein (e.g. nearby bulky and charged side-chains, H-bond donors/acceptors) alter their conformation and electrostatic potential, which is related to their excited-state thermodynamics and excited-state half-life [27]. Further, such interactions actively regulate the mutual orientation of several cofactors, which collectively act as antenna and electron-transfer chain [28].

Cobalamines are corrines, lacking a *meso*-carbon (the carbon corresponding to the methine bridge), and with a varying number of saturated positions at the imidazole termini [29]. As suggested by their name, they generally coordinate a cobalt ion, which is selected for the reactivity of its organometallic complexes. Coenzyme B12 is the active cofactor in various isomerases and methyltransferases, in which cobalt ion is axially bound to an active methide [30].

Nickel is bound to the factor F430, the most reduced tetrapyrrole ring found in living organisms, and highly substituted on pyrrole β-carbons [31]. It is bound to the methyl coenzyme M

reductase, where it is involved in methane release/oxidation process, depending on the hosting organism, by cycling through highly reactive nickel(I) and nickel(III) species.

The mechanism of altering tetrapyrrole properties in nature most likely finds its quintessence in heme rings, i.e. variously substituted iron-containing porphyrins [14,19,32–34]. They are found in electron transport chains as key redox partners; examples are cytochromes (Cyt) *b5* and *c*, which bear heme *b* and heme *c*, respectively (Figure 2 A,B).

Figure 2. Should be here

While heme *c* is typically involved in electron transfer as *hexa*-coordinated complex [35,36], heme *b* functional versatility is literally "explosive" when it weakly binds or lacks a sixth ligand, in the so-called distal position [37]. This coordination geometry makes heme *b* able to sense and transport small molecules, such as nitric oxide and dioxygen, as observed in myoglobins (Mb, Figure 2 C) and hemoglobins (Hb). In these proteins, dioxygen binding is finely regulated in many subtle ways, such as electronic structure tuning, cooperativity, allostery and collective motions [38–41].

Dioxygen activation, in all its declinations (Figure 3), is most probably the real "specialty of the house" for heme *b* binding proteins [42,43]. A wide set of oxidases [44], peroxidases [45], peroxygenases [46,47], dioxygenases [48], and monooxygenases [49,50] promote a myriad of reactions, either with high chemo-, regio- and stereo-specificity, or in a promiscuous and unselective manner [51–53]. Dioxygen, or its two protons two electron reduced form, hydrogen peroxide, give raise to a series of highly reactive oxygen species, upon binding to iron(II)- or to iron(III)-heme *b* species, respectively [54,55].

Figure 3. Should be here

In peroxidases and catalases, such as horseradish peroxidase (HRP, Figure 2 D), heme *b* reacts with hydrogen peroxide in its ferric resting state. Subsequently, a high-valent ferryl, highly reactive species is formed, which is called Compound I (C-I). C-I may either react with sacrificial reductants as in peroxidases [45,53] to form oxidized or dehalogenated [56] organic molecules, or with hydrogen peroxide itself as in catalases to form dioxygen (Figure 3, light blue traces) [57,58]. An additional hallmark of dioxygen activation involves the regio-specific activation of C-H bonds, preventing the release of any undesired radical by-product [59,60]. The cytochromes P450 (P450s, Figure 2 E), a family of monooxygenases, are able to perform this task in a

controlled way [61]. First, their ferric resting state, a water-bound low-spin *hexa*-coordinated complex, is unreactive, until a substrate molecule binds to its hydrophobic pocket. Such event triggers the protein scaffold reorganization, which, in turn, enables an intricate cascade of events, including variation in the out-of-plane heme distortion, water release, electronic transition from low to high spin, redox potential shift, and finally iron reduction by means of a cognate reductase [62,63]. Subsequent dioxygen binding leads to a C-I similar to that found in peroxidases. Notably, P450 C-I has the unique ability to oxygenate unsatured C-H bonds, through a mechanism known as the "oxygen-rebound mechanism" [64,65]. It consists of a stepwise process involving H· radical abstraction from the substrate, forming a basic, ferryl-hydroxo complex (Compound II or C-II) [66], that rapidly recombines with the substrate radical to yield the hydroxylated product. (Figure 3, green traces).

Indoleamine-2,3-dioxygenase (IDO) and tryptophan-2,3-dioxygenase (TDO) are responsible ~~of~~ for tryptophan oxidation to N-formyl-kyneurine in the catabolic pathway of tryptophan as well as a hallmark of stress-dependent oxidative processes [67]. Differently from P450s, dioxygenases promote the insertion of both oxygen atoms from O_2 into the substrate and none of the oxygenations is mediated by C-I. The insertion of the first oxygen atom occurs from their iron-dioxygen adduct (either a ferrous-oxy or ferric-peroxo species) and generates C-II, which in turn promotes the second oxygenation step [68,69] (Figure 3, orange traces).

Such a striking control over heme reactivity may appear unexcelled, but what happens when a second cofactor is coupled to heme? An additional mononuclear cofactor is found in close proximity of heme in the active sites of nitric oxide reductases (NORs, Figure 2 F) [70] and of heme copper oxidases (HCOs, Figure 2 G) [71]. The former catalyze nitric oxide reduction to nitrous oxide in several denitrifying microorganisms [70], the latter are the terminal acceptor of the respiratory electron transfer chain in eukaryotic bacteria and mitochondrial membranes, performing the four-electron reduction of O_2 to H_2O [72]. While NORs use exclusively heme *b* and bind iron (Fe_B) in their non-heme center with a conserved 3His-1Glu first coordination sphere, HCOs may host different types of hemes (e.g. heme *o*, *a* and *b*) and bind copper (Cu_B) with a tripodal 3His coordination sphere, depending on the organism [73]. Thorough mechanistic studies have been performed for these two homologous classes of proteins [74–79], and few details are still under debate [80–82]. Nonetheless, in both cases protein matrix is able to promote selectivity of one metal over the other and to drive the correct *inter*-metal distance along the various oxidation states of the metal and reaction intermediates [83]. Second coordination shell

interactions drive proton shuttling to generate water in HCOs [84] and to release nitrous oxide in NORs [85]. Further, a unique His-Tyr post-translational modification is found in HCOs, that modulates the affinity and the redox potential of the Cu_B center [86].

A final mention should be given to sulfite reductases (SiR, Figure 2 H) and nitrite reductases (NiR), which share a similar tetrapyrrole moiety [87,88]. The first bears the so-called siroheme, structurally similar to the isobacteriochlorin of F430 cofactor, whose proximal cysteine is bridged to a [4Fe-4S] cluster. The mutual interplay between the two cofactors in SiRs plays a key role in delivering the six electrons needed to convert sulfite to hydrogen sufide [89,90]. The second, also known as Cyt *cd1*, bears a unique tetrapyrrole ring called heme *d1*, which shares the same starting scaffold of siroheme [91]. In both classes of proteins, the cofactors play a functional role, other than structural, in which the planarity and/or the high macrocycle distortion, exerted by the protein matrix, trigger their reactivity and control redox steps [88,89].

2 DESIGN OF HEME-PROTEINS: FROM ELECTRON TRANSFER TO SUBSTRATE ACTIVATION AND TRANSFORMATION

We, and many other colleagues, treasured the precious lessons learned from Nature, in order to construct artificial heme-proteins endowed with specific functions. Some scientists approached this task by synthesizing small-molecule metal complexes, capable of mimicking the spectroscopic features and, to a less extent, the reactivity of the natural counterparts [34,42,92]. Other groups, including ours, tried to practice with the "protein ligand", in an effort to test our understanding of the fundamental mechanisms that drive heme cofactor modulation [33]. This was and still is performed either by engineering natural scaffolds or by constructing entirely new-to-nature proteins [93–105]. These approaches demonstrated to be powerful not only to reproduce and/or optimize the biological functions of heme-proteins, but also to construct artificial metalloenzymes that catalyze reaction with unknown natural counterparts [106,107].

2.1 Engineering natural scaffolds

In the field of natural protein engineering and reprogramming, Mb has been converted to a peroxidase/peroxygenase either by metal exchange and cofactor replacement [108,109], by first coordination sphere modification [110], or by rational optimization of the protein environment [111–114]. The same scaffold has been also reprogrammed for abiological ~~xenobiotic~~ reactions like carbene and nitrene transfer, either by means of metal exchange [115], cofactor replacement [116], proximal-ligand substitution [117], or rational redesign of the matrix [118–120].

Combination of these strategies has led to further and ameliorated results in this endeavour [121,122]. Rational design of the Mb distal site has been adopted to install HCO-like [123,124] and NOR-like [125] active sites, adding a new mononuclear cofactor. These putative Cu_B and Fe_B sites, together with heme, were not only structural and functional mimetics, but were helpful in elucidating key aspects about the activity of their natural counterparts [126–128]. More recently, cytochrome *c* peroxidase (C*c*P) activity was steered toward an active SiR surrogate by installing a [4Fe-4S] cofactor in its proximal site [129].

Huge amount of research has been done on P450s engineering and repurposing. For instance, binding site redesign has been widely adopted for altering substrate specificity and further product outcome in terms of regio- and stereo-specificity [130–133]. Decoy molecule strategy, in which a wisely designed molecule cheats the hosting enzyme [134], activating it and shifting substrate-specificity, has been used to perform peroxygenation [135,136], monooxygenation of gaseous alkanes [137] and benzene [138] also within vial cells [139]. ~~Finally, P450 and Cyt *c* have been reprogrammed through directed evolution to afford amazing xenobiotic reactivities, such as carbene/nitrene transfer and fluorination.~~ Directed evolution has emerged as the method of election for reprogramming P450s and other heme-proteins towards abiological reactivities [106,107]. This approach emulates the natural evolutionary process, by applying random mutations to generate a large set of variants and allowing to select the best-performing proteins among them. Outstanding results have been accomplished by the group of Frances Arnold, who was awarded the Nobel Prize in Chemistry in 2018, and many other scientists have significantly contributed to progress in this field. Laboratory evolved P450s and cytochrome *c* have demonstrated to promote a variety of synthetically relevant transformations, including cyclopropanation [140,141], aziridination [142], amination [143], and carbene insertion into C–H,[144,145] S–H,[119] N–H,[146,118], B–H [147] or Si–H [148] bonds. All these reactions occur through carbene or nitrene transfer from an electrophilic heme-carbenoid or -nitrenoid intermediate to a suitable nucleophilic substrate, following a mechanism that resembles the oxygenation of the same substrates mediated by C-I [149]. Directed evolution has been also applied to alter regio and stereo-selectivity of substrate oxygenation [150–152] and fluorination [153], affording artificial biocatalysts for the enzymatic total synthesis of complex molecules [154,155].

A totally different approach in natural scaffold engineering consists in the use of heme-protein surrogates, obtained through enzymatic cleavage of selected Cyt *c*, also known as

microperoxidases (MPs). MPs contain the fundamental covalent framework of heme *c*, that is the heme cofactor and the short proximal histidine-bearing consensus peptide covalently bound to it through thioether bonds [156]. These features provide them with the minimal structural requirements for hydrogen peroxide binding and activation. Consequently, these small molecules show dramatically increased peroxidase and peroxygenase activities compared to the parent, *hexa*-coordinated, Cyt *c* [157–159]. Though lacking a distal environment, they have been coupled to hosting moieties, like antibodies [160,161], silica channels [162], and metal-organic frameworks [163], in order to improve stability from auto-oxidation and directing substrate/product specificity. Moreover, through metal exchange technique, Bren's lab has shown that CoMP11 is a proficient hydrogen evolution catalyst in water, although with limited total turnover number (TON) [164].

Beside natural porphyrin-containing proteins, several groups have inserted porphyrin-binding sites in non-heme-proteins. Antibodies [165], albumin [166,167] and xylanase A [168,169], thanks to their host-guest abilities, have been proficiently adopted to tune ~~porohyrin-based~~ porphyrin-based catalysis. Using a different engineering approach, two dimeric small scaffolds, VK22, an antimicrobial peptide [170], and Glicophorin A [171], were reprogrammed to bind heme in the membrane environment. Starting with simple *bis*-His ligand design, subsequent introduction of aromatic residues afforded more tight heme binding [172]. Overall these studies on repurposed natural proteins or protein fragments have not only greatly increased our knowledge about metalloporphyrin activity tuning, but gifted us with many new chemical tools, useful and prone to pharmaceutical and biotechnological industries.

2.2 Constructing new-to-nature proteins

As outlined in the previous sections, engineering of native proteins has been successful in the development of artificial heme-proteins [173,174]. This approach has the advantage of accessing the wide library of scaffolds carefully selected by Nature. Native proteins are usually stable enough to tolerate multiple modifications, so that the protein global fold is not significantly affected upon altering or installing a metal binding site [175]. However, the exceptional reactivity and selectivity of native enzymes results from million years of evolution, and much effort is needed to completely repurpose a native protein towards a different functionality [104]. Directed evolution techniques have demonstrated to be very successful to this aim, by mimicking and speeding up the evolutionary process [106,176]. Instead of retracing the evolutionary pathway

backwards, we and other groups opted to tackle the heme-protein design starting from the foundations, by creating de novo proteins [177–179]. Though the number of scaffolds that can be designed with a high degree of confidence is limited [180], the major advantage of de novo design consists in providing us with a completely white canvas. The lack of any pre-existing structure represents the unique opportunity to shape the macromolecular host around a metal cofactor, being completely free from any bias of a template native scaffold [181].

Besides the first reported examples, in which metalloporphyrin acted as a template to assist protein folding [182,183], one possible way to engineer heme binding site into new-to-nature proteins is to adopt a combinatorial approach. Several authors used a binary patterning strategy from four-helical bundle miniproteins, alternating hydrophobic and hydrophilic residues according to α-helical periodicity [184,185]. Though successful in installing an heme-binding site and eventually peroxidase activity [186,187], this approach had limited results in terms of success-rate and catalytic activity, especially when compared to rational design of natural proteins. Nevertheless, these proteins could be improved via directed evolution [188], thus demonstrating that folded proteins may have stochastically appeared along the evolution, but at the same time Nature could have explored a much more ample portion of the sequence-structure space [178,189].

Dutton and DeGrado took the design of heme-binding four-helical bundles to a different level [190]. As for previous attempts, when computational approaches were still at their infancy [191–193], fundamental design principle was binary patterning into sequences segregating hydrophobic residues in a four-helix bundle core. Heme cofactor binding, which could also drive the peptide scaffold self-assembly, seemed the logical consequence of such design principles. First attempts relied on parallelly oriented disulphide bridged peptides holding two histidine residues in front of each other, resulting in either mono or *bis*-heme binding [194,195]. Even this simple approach resulted in high and low spin hemes ranging from -230 to -75 mV redox potential. Later on, Dutton considerably redesigned his ‘maquettes’ into stable highly-expressed monomeric proteins, accessing ~~to~~ several functions including dioxygen sensing [196], and photo-induced electron-transfer [197,198]. More recently, Anderson and coworkers, starting from a heme *c* bearing maquette [198], firstly installed peroxidase activity by rationally designing key mutations [199], thus affording C45 protein. Next, they demonstrated that C45 is also endowed with stereoselective carbene transferase activity, being the first-ever enzyme able to catalyze the ring-expansion of pyrrole to ethyl nicotinate, a NADH (nicotinamide adenine dinucleotide) precursor,

in living cells *(E.coli*) [200]. Despite being very active proteins, no structural characterization could be afforded so far on maquettes, limiting their structure-to-function correlation studies. Only one construct was crystallized and characterized, even though any preorganization of the scaffold towards heme-binding could be observed [201].

Our group also exploited the four-helix bundle scaffold in the development of MiniPeroxidase 3 (MP3) [202]. It represents one of the first example of a de novo designed proteins able to accommodate a *penta*-coordinated heme, endowed with peroxidase activity. MP3 was patterned after the heme-facing helices of Bacterioferritin (Bfr). The original sequence of Bfr was modified to engineer an asymmetric α_2-heme-α_2 covalent sandwich. The HRP proximal and distal site were shaped, resulting in an artificial peroxidase, provided with high catalytic turnover and efficiency in the ABTS oxidation by H_2O_2.

DeGrado and colleagues have developed a large number of four-helical bundle scaffolds able to tightly bind different types of abiological porphyrins with variable stoichiometry [203–205]. Their structural approach was relying on backbone parametrization of the four-helical bundle, originally based on diheme-binding cytochrome from Cyt *bc1* complex [206]. The design afforded very well-behaved proteins, with high affinity for their cofactors [204], and suitably located second sphere interactions. This approach also led to the first de novo heme-binding membrane protein [205]. Unfortunately, high-resolution structural characterization could not be performed. Only recently, high-resolution NMR structure of the apo and holo PS1 protein, a newly developed scaffold, has been obtained [207]. Notably, PS1 structure is in sub-angstrom agreement with the design. This outstanding result could be achieved thanks to a cleverly developed strategy, inspired by numerous natural proteins (e.g. Cyt *b5*) [208,209], which involved the design of a highly-stable folded domain able to host an abiological cofactor. Finally, they showed that tightly bound zinc *m*-tetrakis(trifluoromethyl)porphyrin could be photoexcited, and its excited state undergoes radiative decay, as when dissolved in organic solvent [207].

De novo-designed beta-sheet proteins are less frequent than helices, due to their intrinsic propensity to aggregate [210–212]. However, heme cofactors in Nature may be found in beta folds [213,214]. Several de novo β-peptide scaffolds, able to cage up to 4 hemes *via* His coordination, have been developed [170,215,216]. Poor peroxidase activity was detected, suggesting a strong binding affinities between the iron ion and two axial His ligands. Remarkably, some analogues were soluble and monomeric in solution, allowing the structural

characterization by NMR of the *apo* forms [217]. Unfortunately, the lack of high-resolution structures of the *holo* states did not allow a clear correlation between peptide sequence/coordination geometry and heme binding affinity.

2.3 Miniaturized proteins through helix-heme-helix topology

The use of α-helical peptides able to cage the heme group has been and still remains the focus of the majority of the works in the field, as the α-helix motif is a recurring structural motif that surrounds heme in numerous natural proteins. Along these lines, we approached the goal of obtaining minimal heme-proteins endowed with activity by sandwiching the porphyrin ring between two flanking helices [218].

Contemporary and independently from us, few other groups elaborated similar systems [33,219,220]. Their focus was primarily to dissect specific aspects of heme-protein properties, such as: (i) the contribution of histidine coordination on protein folding and heme redox potential [221,222]; (ii) the role of hydrophobic interactions between heme and the peptide environment on folding [223–226]; (iii) the role of helix stapling on heme binding either by disulphide bridges and N-capping motifs [227–229]. We tried to combine all these elements in a single well-designed/behaved synthetic miniprotein, by using a miniaturization approach based on a different process and objectives. The design process (i) was driven by a structural hypothesis and it was inspired by the inspection/miniaturization of a natural protein; (ii) was aimed at finding the smallest scaffold able to reproduce the minimum set of structural interactions leading to the variety of functions observed in Nature; (iii) became incremental, step-by-step adding functional requirements, once a tunable and reliable scaffold was obtained [104,230].

An essential requirement for the miniaturization approach we adopted is the prior knowledge of the structure to be reproduced. When we started the design of our scaffold, structurally characterized heme-binding proteins were limited to Hb, Mb, few Cyt *b* and *c*, C*c*P, and the earliest structures of P450s. Among them, Hb was the most widely studied [231]. In particular, we focused on the helical hairpin (helices E and F) surrounding the heme (Figure 4 A,B), which is partially solvent exposed, and thus prone to be "excised" from the whole protein.

Figure 4. Should be here

Differently from microperoxidases [156], we did not simply intend to obtain an "extracted" system, but rather to elaborate a more general design protocol, which consisted in decreasing

complexity by increasing symmetry [230,232]. To this end, the most reasonable choice appeared to symmetrize the short and amphipathic F-helix bearing the proximal histidine ligand. This helix seemed sufficiently long to cover the whole porphyrin and almost perfectly parallel to its plane, thus simplifying the choice of heme-facing residues. We opted for a covalent linkage between the porphyrin and the peptide moieties, to compensate for the loss of numerous interactions that the heme cofactor entertains with the hosting protein. Taking into account only the F-helix from the B chain of human deoxyhemoglobin (pdb id: 2HHB), we found out that the sequence comprising nine residues, from Leu88 to Leu95 (Figure 4 B), was sufficient to cover the heme. A docking moiety was now needed, and Lys95, at the i + 3 position from His92, seemed a good target, as it lays in close proximity of the heme propionate (Figure 4 C). Simple rotamer search allowed carboxyl propionate and Lys ε-amino functional groups to be at bonding distance (Figure 4 D). Most of the heme facing residues was conserved, unless for Glu90 and Asp94, that were replaced by the neutral Gln and Asn, respectively, and for Ser89 and Cys93, that were replaced with Ala, because of its higher helical propensity [233] (Figure 4 E). Acetyl and amide groups were added at each *terminus* to avoid helix-destabilizing interactions. Deuteroporphyrin IX, lacking the reactive vinyl groups, was preferred over protoporphyrin to overcome synthetic difficulties, preserving ring asymmetry that would drive stereo-specific interactions. This design process afforded half of the final backbone of the miniaturized protein. Through a C_2 operation along the pseudo-symmetry axis, lying along α and γ *meso* porphyrin carbons, the helix–heme–helix sandwich was obtained (Figure 4 F and Scheme 1).

Scheme 1. Should be here

The iron complex of Mimochrome I (FeMC1) was thoroughly characterized, and its spectroscopic features indicated that a *bis*-His coordination environment was indeed achieved, and that, upon histidine deprotonation and concomitant metal binding, the peptides correctly folded in α-helix [218,234].

Despite these encouraging results, which supported the design principle, a complete structural characterization was intrinsically inhibited due to poor solubility and very low helical content of the miniprotein, without the addition of the helix-inducing solvent 2,2,2-trifluoroethanol (TFE). This undesired effect was ascribed to weak iron coordination by histidine residues, which underwent protonation equilibrium, even at pH 7. This finding caused peptide flexibility, porphyrin exposition to the solvent and subsequent aggregation. Nevertheless, such flexibility allowed for some unexpected reactivity; similarly to heme-peroxidases a small amount of high-

spin iron was found, thus making FeMC1 able to catalyse styrene epoxidation for few turnovers [234].

In order to stabilize the structure of MC1, we replaced the metal ion. Indeed, Co(III)-Mimochrome I (CoMC1) not only was highly soluble (up to mM concentration), but showed enhanced helical folding respect to FeMC1 [235]. This was ascribed to the higher affinity of the low-spin d^6 cobalt(III) ion toward nitrogen-donor ligands. This dramatically decreased the His pKa, stabilizing the sandwich down to pH 2, and inhibiting ligand-exchange. The enhanced stabilization of the cobalt complex allowed us to identify and isolate two distinct diastereomeric species, presumably also present in the iron complex in a fast interconversion equilibrium. These two species, namely Δ and Λ diastereomers, showed opposite Cotton effect in the Soret region, with negative and positive signs, respectively. These spectroscopic signatures would correlate with two opposite heme distortions [236,237] (Figure 5). Indeed, opposite sign of the Cotton effect was observed for isomers A and B of Mb, which differ by a 180° heme flip in the binding pocket [238]. CoMC1 Δ and Λ diastereomers were stably folded, thus readily characterized by NMR spectroscopy, representing the first designed heme-protein structure ever determined [235] (Figure 5).

Figure 5. Should be here

Retrospectively, the two structures appeared to be quite different, the two main differences residing in the mutual histidine angle (called β angle: 30° for Δ, 75° for Λ), and the tilt angle between the helix and the porphyrin plane (~180° for Δ, ~30° for Λ). Interestingly, Δ isomer was closer to the designed model from Hb F-helix (Figure 4 F), though Λ isomer was strikingly similar to a putative dimer of slightly translated E-helices that enables metal binding.

One design possibility to solve the problem of the diastereomeric equilibrium would be substituting deuteroheme with more symmetrical porphyrins [225]. However, we decided to tackle this design challenge using close-to-natural deuteroheme for two reasons: (i) to direct the desired peptide folding by positive and negative design principles, in order to deeply understand how Nature drives selective heme binding; (ii) to better modulate heme distortion, as in natural proteins, thus unraveling the influence that opposite Δ and Λ configuration may have on catalysis. We therefore envisaged two orthogonal approaches. Based on CoMC1 structures, we rationalized that while Δ isomer was keeping the desired hydrophobic interactions (among Leu residues and the porphyrin ring), the Λ isomer was much looser, with helix head and tail lying out of the

porphyrin. In the design of Mimochrome II (MC2, Scheme 1) we therefore tried to stabilize Δ diasteromer. The helices and their hydrophobic pattern were conserved, and further stabilized by adding N- and C- capping motifs, and thus elongating the structure up to 14 residues [239]. At the N-*terminus* an Asp may both contribute as H-bond acceptor from unpaired backbone N-H groups or stabilize helical dipole [240]. At the C-*terminus* a Lys residue was added as C-capping, and a simple extended Ile-Thr-Leu motif, that may enhance hydrophobic coverage of the heme. This design solution endowed FeMC2 with increased solubility, higher helical content and a marked propensity towards Δ configuration, as evidenced by the negative Cotton effect of the Soret band [239].

In order to stabilize Λ diasteromer, we speculated that less design effort would actually be needed: (i) Leu residues should be mutated to more polar side chains as they are more solvent exposed in the Λ configuration; (ii) considering that both helix ends fall out of the porphyrin ring, insertion of *inter*-chain salt bridges should positively impact structural stability, both by helix-dipole interactions and by negative design principles, that would destabilize competing topologies [178,241,242]. MC1 Ala residues were mutated to Ser and the hanging Leu1 and Leu9 to Glu and Arg, respectively. The devised substitutions resulted in Mimochrome IV [243] (Scheme 1, MC4). This strategy was successfully as FeMC4 was not only well-behaved, both in terms of solubility and helical content, but it adopted the unique Λ configuration, as shown by Circular Dichroism. Most importantly, CoMC4 was structurally characterized by NMR spectroscopy. The structure revealed that the overall design target was achieved: only Λ isomer was present in solution; helices were flanking at almost 30° tilt to the deuteroheme plane; histidine mutual dihedral angle was of ~52°; designed head-to-tail *inter*-chain salt bridges were confirmed by restrained molecular dynamics (RMD) (Figure 6 A). Subsequently, MC4 crystal structure was also solved [244]. It confirmed the overall topology, and helix/porphyrin tilt angle, even though the designed head-to-tail salt bridges became *intra*-chain in the crystal. Moreover, *bis*-His first coordination sphere showed a slightly increased in the mutual dihedral angle (57°, Figure 6 B). Further, the two helices were covering only half of the porphyrin ring, thus leaving a very wide hydrophobic area totally exposed to the solvent. Though few variations in the structure could be envisaged for such a small protein upon crystal packing interactions, we were interested to figure out which of the two structures might be predominant in solution when iron was in place of cobalt. More recent results, by paramagnetic NMR Fermi contact shifts on FeMC4, pointed out

that the NMR model was indeed more representative of the actual iron coordination in solution [245].

Figure 6. Should be here

The low His pKa value observed for FeMC4 in the oxidized Fe^{3+} form (N^{ε} pK_{app} ≈3.8) confirmed the strong *bis*-His character of this miniprotein, with an even more strong His-Fe coordination in the reduced Fe^{2+} form (N^{ε} pK_{app} ≈3) Noteworthy, the different imidazole His pKa values, found for Fe^{3+} complexes of MC1 and MC4 (2.5 and 3.85, respectively), was attributed to a more polar environment around the His residues in MC4, as a result of the substitution of the hydrophobic Leu1 and Leu9, with Glu and Arg, respectively.

Interestingly, FeMC4 behaved as a mid-potential Cyt *b* [246], given that its redox potential lies at -80 mV when tested by protein film voltammetry [243]. This finding, together with the observed modulation of the His pKa value upon residue substitution, confirmed that the minimal MC scaffold works as a well-behaved synthetic miniprotein. Further, the simple structurally defined FeMC4 model provided an excellent opportunity for exploring the subtle mechanisms that control heme functions. Thus, we used FeMC4 to verify if its functionality, in terms of redox potentials, would be modulated by residue substitution as observed in natural heme-proteins [220]. We therefore synthesized two MC4 analogues, namely Mimochrome IV 8Lys and Mimochrome IV 8Glu (MC4K, MC4E, Scheme 1). These two analogues bear four mutations on each peptide chain, in positions 2, 3 and 6, 7, either to four positively-charged Lys residues or negatively charged Glu [247]. Despite the expected destabilization that could be envisaged by the high number of charged residues on the helix surface, both synthetic models were showing the same spectroscopic properties and iron complex stability, as His acidity has been directly correlated to metal complex inertness to ligand exchange (Table 1). In FeMC4K, the observed pK_{His} value was 2.6, lower than the 3.8 value from both FeMC4 and FeMC4E. As expected, redox potentials for iron reduction follow the order FeMC4K > FeMC4 > FeMC4E, the last being very stable in the iron(III) oxidation state. MC4 scaffold was therefore able to almost span the full range of redox potentials of Cyt *b* family. However, it was not possible to drift the potential up to positive values, probably because of the histidine exposition to the solvent, or for possible second-shell interaction with the Glu in position 1 as observed in CoMC4 crystal structure. Such interaction would give to histidine a histidinato character, thus stabilizing the metal oxidized state [243].

Table 1 should be here.

Thanks to the results obtained and its versatility in tolerating several mutations, MC4 significantly contributed to our understanding of the determinants driving heme binding, metal coordination, helix stabilization, and redox potential modulation in natural proteins. This was mainly possible thanks to the available atomic-resolution experimental structures, which allowed the necessary structure-to-function correlation. These results are even more striking when considering that CoMC4 and the disulphide-bridged cyclic peptide Cy-AAEK from Suslick group [227,228] (in complex with the highly symmetric cobalt-coproporphyrin I) have been the only fully de novo structures binding a porphyrin-based cofactor deposited in the PDB (Protein Data Bank) until 2017 [207], as well as the first and only X-Ray deposited structure till 2018 (a still not published multicofactor maquette by Moser and Dutton).

The important lessons learned so far with *bis*-His compounds were used to guide the design of *penta*-coordinated analogues, endowed with activity in oxidation catalysis (Figure 7).

Figure 7 should be here.

Our goal was not only to develop a small yet functional peroxidase, but also to evaluate the contribution that the distal peptide may give in catalysis [33]. We started by using the Δ stereoisomer and adopted a combination of the previous strategies to stabilize helical folding. In particular, the proximal peptide of Mimochrome VI (MC6, Scheme 1 and Figure 7 A) was patterned after the tetradecapeptide chain (*TD*) of MC2, with the main difference being the inclusion of Glu2 and Arg10 residues to afford the head-to-tail *inter*-chain ion pairs, observed in MC4 (Scheme 1). The distal chain was made up by a decapeptide (*D*), featuring a Ser in position 6 in place of the metal-binding His, to create a vacant distal side. Moreover, the *D* chain houses Glu in position 2 and Arg in position 10 to satisfy ion pairs, and an Asp N-capping residue in position 1. For both peptides Gln, was placed in position 3 instead of Ser (previously in position 2 for MC4), to avoid undesired off-pathway N-capping, as observed in MC4 crystal structure. This asymmetric analogue, the first of the Mimochrome series, displayed unprecedented functional features [250]. Fe(III)-MC6 was indeed able to activate H_2O_2 and showed Michaelis and Menten kinetic in the oxidation of several organic substrates, displaying multiple turnovers and catalytic efficiency (k_{cat}/K_m) in the range of natural HRP. Peroxidase activity was observed towards ABTS and guaiacol, as well as nitration of phenols in ortho- and para-positions, most likely through phenoxyl radical formation. It is worth to notice that maximum catalytic activity was observed upon TFE addition. TFE addition also increased helical content and drifted the diastereomeric

equilibrium towards the desired Δ configuration. Moreover, when compared with the monoadduct, lacking the distal decapeptide, Fe(III)-MC6 showed lower TOF (k_{cat}) but higher TON in the presence of 50% TFE, whereas higher TOF and TON were observed in the absence of TFE (Figure 8 A, B).

Figure 8 Should be here

Altogether, these results suggested that a well-folded miniprotein is needed for endowing the cofactor with high activity, and in particular: (i) the distal *D* peptide organization over the porphyrin ring negatively influences k_{cat}, probably because the metal site is more hindered; however, it dramatically increases the TON, thus exerting a protective effect toward degradation; (ii) the proximal *TD* helix has a positive influence on k_{cat}, which is clearly related to tighter His binding to the heme. This last finding was recently confirmed by Hilvert and co-workers, through heme-protein engineering. Indeed, the introduction of a noncanonical N^{δ}-methyl histidine (NMH) as the proximal ligand endows Mb with efficient peroxidase activity [110] and dramatically increases TON of ascorbate peroxidase (APX) [252], likely as a consequence of the stronger electron-donating effect of NMH compared to the N^{δ}-hydrogen-bonded histidine.

FeMC6 was completely characterized, and spectroscopic and electrochemical analyses were performed to evaluate both spin state of the iron and the Fe^{3+}/Fe^{2+} redox potential [248,249]. UV-Vis analysis suggested that ferric MC6 could be in the high spin (S = 5/2) spin state, however Resonance Raman spectroscopy suggested that it could be best described as an admixed state (S = 3/2, 5/2) [249], as already observed in Cyt *c'* and in artificial peroxidases [253,254]. The generation of this electronic state was recently supported by a QM-MM (quantum mechanics/molecular mechanics) analysis [255]. Electrochemical analysis was performed on FeMC6 either when adsorbed on electrode surface or freely diffusing in solution (Table 1). The E°'(Fe^{3+}/Fe^{2+}) were found ranging from -111 mV on ITO (indium titanium oxide) electrode to -99 mV in diffusion (versus SHE). The redox potential value is higher than those of most peroxidases, suggesting very high oxidative power of the C-I and C-II species. ~~/Fe^{3+} couple.~~[256–258] Indeed, it has been established that the molecular factors that determine the E°'(Fe^{3+}/Fe^{2+}) values, also affect the redox potentials of the C-I/Fe^{3+}, C-I/C-II and C-II/Fe^{3+} redox couples, which are relevant for catalysis.[259] ~~In this respect, an~~ An existing linear correlation between the redox potential of the E°'(Fe^{3+}/Fe^{2+}) and the C-II/Fe^{3+} couples has been demonstrated for a variety of heme-proteins [260], allowing to extrapolate a value of ~1.17±0.07 V for FeMC6. Such value would be higher than that HRP (0.9 V) but still lower than those of high-potential peroxidases

able to oxidize manganese ($E°(Mn^{3+}/Mn^{2+})$ = 1.5 V) [261]. Finally, it was found that FeMC6 was able to catalyze dioxygen reduction from the ferrous state, when immobilized onto gold electrodes [248].

Potential interest as industrial enzymes prompted us to test the applicability of this construct upon immobilization to obtain catalytically active nanomaterials. In principle, thanks to its very small size (radius of gyration ~1 nm compared to HRP ~ 3 nm), this minienzyme grants with the possibility of drastically increase the specific activity of functionalized nanomaterials [262], by increasing the active-site density. Therefore, FeMC6 Ser6Gly analogue was directly immobilized on gold nanoparticles (AuNPs), after being functionalized with lipoic acid [251] (Figure 8 C). The nanocomposite retained peroxidase activity; however, a decreased catalytic efficiency was observed. AuNPs characterization let us to ascribe the observed drop of activity to both the formation of a double layer of FeMC6 Ser6Gly on the AuNP and possible to unfavourable negatively charged environment. Redox potential evaluation of this derivative on gold electrode gave a more negative E°' of -143 mV, thus suggesting a less active C-II species [252,260].

The successful design of MC6 further supported the versatility of MC minimal scaffold, being able to incorporate a functional heme. Therefore, we proceeded with several rounds of MC6 redesign, to increase its catalytic activity, in order to make it an industrially feasible synthetic alternative to natural peroxidases (Figure 7). Modification of the peptide scaffold started by evaluating the role that the head-to-tail ion pairs were playing on function. Four analogues were then synthesized, in which apolar Leu residue was replacing either one of the four residues involved in the salt bridges, i.e. Glu2 and Arg10 either from *TD* or *D* chains. Leucine was chosen in order to compensate salt-bridge removal, thus re-establishing the interaction observed in MC1 [263]. The best performances in terms of catalytic activity were observed for Fe(III)-Glu2Leu(*TD*)-Mimochrome VI (Fe(III)-MC6*, Scheme 1 and Figure 7 B), which showed 2-fold increase in TOF and catalytic efficiency toward hydrogen peroxide catalyzed ABTS oxidation. Based on the FeMC6 model, and guided by the structural characterization previously performed, we hypothesized that breaking the Arg10(*D*)-Glu2(*TD*) interaction, upon Glu2Leu mutation, would actually cause "freeing" Arg10 (Figure 9 A). The "free" Arg10 side chain, in turn, could serve as H-bond donor, thus resembling Arg38 of HRP [264] (Figure 9 B), which is known to assist hydrogen peroxide activation and C-I/II stabilization. Indeed, the spectroscopic characterization of the isolated Fe MC6* C-I derivative confirmed this hypothesis [263]. As a

further support, theoretical analysis identified the Arg10(*D*)-Glu2(*TD*) as the weaker among the four ion pairs occurring in MC6 analogues [255].

Figure 9 should be here.

MC6 and MC6* demonstrated that even these small-sized proteins may recover the features of natural proteins, together with their complex interplay of factors that determine catalysis. The study of these compounds taught us three important lessons. Firstly, the design of a *penta*-coordinated high-spin iron complex is mandatory to endow heme with peroxidase activity, and, very important, helical folding of the proximal chain is crucial in correctly position the coordinating His. Secondly, as observed for natural heme-proteins, the presence of a correctly designed distal pocket is crucial to drive substrate binding, modulate catalyst activity and most importantly its stability toward degradation during catalysis. Finally, such a small catalyst is strongly influenced by the environment, either in diffusion or immobilized on solid supports or nanomaterials. This aspect may be successively considered for maximizing activity, by proper selection of the hosting matrix.

3 MIMOCHROME VI*A AS A GENERAL-PURPOSE SCAFFOLD

Lessons learned from the development of *penta*-coordinated Mimochromes made us much more confident in how to tune catalyst properties, by introducing specific modifications in the peptide scaffold. As the Glu2Leu(*TD*) mutation in MC6 allowed to greatly enhance catalytic efficiency in peroxidase activity [263], the next-step was to improve the robustness of the scaffold. Our studies with MC6 highlighted that the presence of the distal peptide is critical in dictating catalyst stability, acting as a shield against self-degradation, thus prolonging catalyst lifetime [250]. Along these lines, we hypothesized that better shielding could be obtained by making the *D* chain more prone to adopt a stable helical folding and to interact with the metalloporphyrin ring. To this end, we took this challenge by altering the plasticity of the *D* chain, as well as its hydrophobicity [266].

Taking advantage of our expertise in using noncoded α-amino acids as conformational constraints [267], the simplest Cα,Cα-disubstituted amino acid, 2-aminoisobutyric acid (Aib, U), was selected to reduce backbone flexibility and to stabilize helical folding [268,269]. The presence of two methyl groups at Cα of the Aib produces severe restrictions on its conformational freedom. As a consequence, the formation of α-helical secondary structures is strongly favoured for Aib-containing peptides.

Two Aib residues were incorporated in the sequence of the *D* chain, in order to create a hydrophobic patch, which would enhance peptide-porphyrin interaction. Only the pairs of residues on the same side of the helix (i , i + 4) were considered in the search for the best positions for mutation. Asp1, Glu2, Ser6, Lys9 and Arg10 were excluded from the screening, as these residues were structurally or functionally essential. The helix-forming tendencies of each amino acid were considered in order to obtain the sequence with the highest helical stabilization [233]. Based on this analysis, positions 3 and 7 were chosen for mutation and the Q3U, S7U decapepetide was employed in the design of the new analogue, named MC6*a (Scheme 1 and Figure 7 C). According to the designed model, both Aib side chains are facing towards the deuteroheme.

The beneficial effect of Aib insertion on the secondary and tertiary structure of the complex was proven by a comparative spectroscopic analysis in solution of FeMC6*a and its precursor, FeMC6* [263]. Whereas both analogues appear poorly structured in aqueous buffered solution, FeMC6*a experiences a much higher increase in the helical content upon addition of TFE, as revealed by CD spectroscopy in the far-UV region. Concurrently, the enhanced Cotton effect in the Soret region suggested a stronger interaction between the porphyrin and the peptide chains in the new analogue. The stabilization of the sandwiched topology by Aib residues was also supported by NMR data from the diamagnetic Co(III)-derivative of MC6*a. In particular, both U3 and U7 methyl groups displayed lower-than-average chemical shifts, which were reasonably associated to a hydrophobic interaction with the porphyrin [266].

The above structural finding clearly suggested MC6*a to behave differently from its predecessors. This prompted us to, exploit MC6*a as a scaffold for hosting and tuning the activity of different metal ions, with the aim of expanding the range of its applications beyond just peroxidase catalysis. Accordingly, its iron, manganese and cobalt complexes of have been screened towards different reactivities.

3.1 Iron and Manganese: from peroxidase to peroxygenase activity

Peroxidase-like activity of FeMC6*a was examined and compared to the parent analogue, FeMC6*. When screened as catalyst for ABTS oxidation, FeMC6*a performed more than a doubled number of turnovers compared to its precursor (Table 2, entries 1 and 2). Considering the established relationship between TON and the protective role of the distal peptide chain, this result could be considered as a proof of concept that introducing Aib residues into the *D* chain

favours its interaction with the porphyrin. The improved hydrophobic character of the *D* chain in MC6*a also leads to the narrowing of the active site cleft, which results in lowered affinities (higher K_m) for both H_2O_2 and ABTS. This effect is perfectly counter balanced by an increased k_{cat} for FeMC6*a, leading to similar catalytic efficiencies (k_{cat}/K_m) for the two catalysts [266].

Table 2 should be here.

Overall, FeMC6*a is the best artificial peroxidase reported to date, working in the presence of 50 % TFE and displaying a 20-fold higher catalytic efficiency against ABTS with respect to HRP (Table 2). This exceptional reactivity represents a real opportunity for a number of practical applications. The reduced size of our catalyst compared to natural peroxidases, coupled to the easy scale-up of its synthetic route, offer significant advantages for use in the construction of bio-inspired sensors and nanomaterials.

These achievements prompted us to evaluate the versatility of the MC6*a scaffold towards metal replacement, by swapping iron to manganese. The latter was chosen owing to the well documented catalytic promiscuity of Mn-porphyrin complexes, spanning from superoxide dismutase [270–272] to unsaturated C-H halogenation [273–275] or hydroxylation [109] activities. Upon reaction with peroxides, Mn-porphyrins have been shown to access both the Mn^{V}-oxo and the Mn^{IV}-oxo states [276–278]. The former has been proposed as the active oxidant in the oxygenation of a number of unactivated substrates, similarly to ferryl-oxo Compound I of P450 enzymes [279,280]. Mn^{IV}-oxo species have instead attracted less interest in catalysis due to their limited reactivity. When iron is replaced with manganese in native heme-proteins, a substantial drop in their oxidative activity is commonly observed [281–283]. This is due to the predominant stabilization of Mn^{IV}-oxo species in biological catalysts, and indeed rational engineering of the protein matrix [284,285] and/or the porphyrin cofactor [108,109] is required to make them functional.

The spectroscopic features of MnMC6*a closely match those of Mn-reconstituted HRP, both in the resting and high-valent states (Figure 10 A), thus suggesting a protein-like behaviour of this complex. This is not unexpected, considering that also the UV-Vis spectra of FeMC6*a (Figure 10 B) resemble those of HRP both in the ferric and ferryl-oxo states.

Figure 10. Should be here

Notably, MnMC6*a-derived C-I exhibits marked reactivity, with respect to HRP manganyl-oxo species, which is exceptionally stable and inert towards external substrates. MnMC6*a, as well as its iron congener, was screened for peroxygenase-like catalysis, using the H_2O_2-mediated thioether sulfoxidation as test reaction. Both FeMC6*a and MnMC6*a complexes demonstrated to efficiently promote the selective conversion of phenyl thioethers into the corresponding sulfoxides, with experimental evidences of a direct oxygen-transfer mechanism [286]. Thioether oxidation by Mn- and FeMC6*a shows a pH-dependency that closely resembles that of peroxide activation, thereby suggesting the involvement of the ferryl or manganyl-oxo species in the reaction. The optimal pH value for MnMC6*a (pH = 10.0) was found to be 3.5 units higher with respect to FeMC6*a (pH = 6.5), reflecting the lower Lewis acidity of Mn^{3+} compared to Fe^{3+}. This property is also responsible for their different abilities to promote metal-bound water deprotonation (pKa = 9.8 and 6.9 for Mn- and FeMC6*a, respectively). It is worth to note that peroxide activation and water deprotonation occur at lower pH values for MC6*a catalysts than for the corresponding metal derivatives of peptide-porphyrin conjugates with a fully solvent-exposed distal site, as microperoxidase 8 (MP8) [287]. The hydrophobic environment created by the distal peptide chain around the metalloporphyrin could reasonably modulate the electronic properties of the metal centre, besides providing catalyst with a shielding against self-degradation. In this respect, Fe- and MnMC6*a are among the most robust artificial metalloenzymes for thioether sulfoxidation, largely exceeding the turnover numbers of their competitors, either when considering natural, reconstituted or engineered proteins housing synthetic cofactors (Table 3).

Table 3. should be here.

The reactivity of Fe- and MnMC6*a towards peroxygenase-like reactions is far higher when compared to native and Mn-reconstituted HRPs. The low reactivity of the native enzyme could be certainly ascribed to an effect of the protein matrix, which was selectively tuned for the activation of peroxide rather than the oxy-functionalization of organic substrates. Differently from natural enzymes, the lack of a specifically evolved active site endows these miniaturized systems with an intrinsic versatility and opens new avenues towards new enzymatic or abiological reactivities. Exploiting of the oxygen transfer reactivity of our catalysts towards reactions with potential synthetic interest is currently ongoing in our laboratories, and further investigations will be devoted to completely carve out the catalytic potentialities of Fe- and MnMC6*a complexes.

3.2 Cobalt: hydrogenase activity

Whereas iron and manganese are the leading candidates for oxidation chemistry, cobalt has appeared as the metal of choice for energy-related catalysis [293]. Many efforts in this field have concerned with the development of efficient and stable catalysts for the hydrogen evolution reaction (HER) [294–298]. Hydrogen (H_2) represents a sustainable and renewable energy source, which could be directly obtained from water. Nature's answer for H_2 demand involves hydrogenase enzymes [299]. The latter are the most efficient catalysts for HER, promoting reversible proton reduction in water with low overpotentials [300]. However, hydrogenases are complex biochemical machineries and their practical application in scalable H_2-production meets difficulties associated with their production on a large scale and their sensitivity to molecular oxygen, which rapidly inactivates these enzymes [301]. Therefore, significant efforts have been devoted to developing functional hydrogenase mimics, more suitable to manipulation and screening than native hydrogenases [294–297]. In collaboration with the Bren's group, we have screened the Co-derivative of MC6*a as a potential electrocatalyst for HER. To date, numerous synthetic or protein-based cobalt complexes have been studied for this kind of reactivity [302–307]. High overpotential values, low water-solubility and the need for strong acids as proton sources are the common drawbacks associated with small-sized complexes [308–310]. On the other hand, cobalt-reconstituted heme-proteins, such as Mb and Cyt *b562*, have been shown to function in neutral water, but suffering from O_2-intolerance and unsatisfactory TONs (up to 1500) [311,312]. As an exception, cobalt-Cyt *c552* from *Hydrogenobacter thermophilus* (Ht-CoM61A) displayed exceedingly high TON (270 000), albeit with a high overpotential value (730 mV) [313]. Being in the middle ground between biological and small-molecule catalysts, CoMC6*a appeared suitable for this challenge. Indeed, differently from previously reported metalloporphyrin catalysts, CoMC6*a efficiently promotes HER in neutral water and in the presence of molecular oxygen [314]. Studies conducted by Bren and co-workers on Co-Microperoxidase11 (CoMP11) [164] allowed a comparative analysis between the two peptide-porphyrin conjugates, underlining the effects of the peptide scaffold on the catalytic performances. CoMC6*a displayed similar overpotential and turnover frequency to CoMP11, but demonstrated to retain its activity for several hours, leading to a 9-fold increased TON (up to 230 000 for CoMC6*a compared to 25 000 for CoMP11). The remarkably higher robustness of this complex has been ascribed to the shielding effect of the *D* chain, which protects the catalyst against degradation. Furthermore, TFE-driven peptide folding was found to beneficially affect the

overpotential of CoMC6*a, inducing a 90 mV shift towards less negative values. The correlation between peptide folding and overpotential becomes clear from an inspection of the TFE-dependent cyclic voltammetry experiments with CoMP11 or CoMC6*a (Figure 11). Indeed, whereas a decrease of the peak current is observed for both catalysts, only CoMC6*a experiences a shift in the peak potential for hydrogen evolution.

Figure 11. Should be here

The decrease of the peak current observed at increasing TFE concentrations could be reasonably ascribed to a different solvation effect of the organic solvent, which limits the accessibility of protons in proximity of the catalysts [315]. The shift in the peak potential could be rationalized as a combination of effects derived from the structural organization of the MC6*a scaffold. When arranged into a sandwiched structure, the *D* chain could provide a more hydrophobic environment around the metal center, tuning its redox potential and thereby lowering HER overpotential. Additionally, the folding of the decapeptide may allow the amino acid sidechains to approach the metal center and assist the proton-coupled electron transfer (PCET) during catalysis. This last phenomenon, also referred as the "hangman effect", has been reported by Nocera and co-workers [309,316] and relies on the assistance by a proton-exchanging functionality positioned in proximity of the metal ion. Considering the designed MC6*a model, Arg10 and Glu2 residues in the decapeptide chain have been supposed to be close enough to exert the hangman effect. Further, our recent studies evidenced that the overpotential is strongly altered by the presence of exogenous proton donors in water, highlighting the importance of PCET in H_2 evolution by CoMC6*a [317]. While the potential is strongly dependent by the pKa of the proton donor, it appears to be unaffected by its concentration. This finding suggests that protonation steps may not be rate-limiting in the reaction mechanism, despite rate-limiting steps in H_2-evolution catalysis often involve the protonation steps [318,319]. This surprising outcome may be attributed to the peptide scaffold playing a role in catalysis, by likely positioning the proton donors for favourable interaction within the active site.

4 CONCLUDING REMARKS

The work described in this review exemplifies the remarkable progress reached over the last two decades in developing miniaturized heme-enzymes. What started as minimal structural mimetics lacking any functionality, has grown into highly reactive metalloenzymes approaching or even surpassing the catalytic performances of the natural counterparts. The Mimochrome family

represents a clear evidence of the reliability of miniaturization in successfully mimicking two of the three Nature design strategies (see Figure 1). Indeed, our design approach allowed hosting the same cofactor (deuterophorphyrin) in a self-sufficient structure, prone to be subjected to metal ion replacement and environment modulation, thus achieving a wide range of functionalities. Though many challenges have been overcome, much work is yet to be done. Additional steps of redesign will be aimed at further optimizing the whole catalytic performances of Mimochrome metal complexes, to exploit their full potential in applicative and industrial process as synthetic heme-enzymes.

5 ACKNOWLEDGEMENTS

The authors thank all former members of the group for their contributions to the results described in this review, and Monica Grasso for help in the final editing of the manuscript.

6 FUNDING

The work from authors' group reported herein has been partially supported by Campania Region "Programma Operativo FESR Campania 2014–2020, Asse 1", [CUP B63D18000350007].

7 REFERENCES

[1] Da Silva, J. J. R. F. *The biological chemistry of the elements: the inorganic chemistry of life.*; 2nd ed.; Oxford University Press: New York, (2001).
[2] Armstrong, F. A. (2008) Philos. Trans. R. Soc. Lond. B Biol. Sci., 363, 1263–1270.
[3] Sánchez, M., Sabio, L., Gálvez, N., Capdevila, M. and Dominguez□Vera, J. M. (2017) IUBMB Life, 69, 382–388.
[4] Davidi, D., Longo, L. M., Jabłońska, J., Milo, R. and Tawfik, D. S. (2018) Chem. Rev., 118, 8786–8797.
[5] Berg, J. M., Tymoczko, J. L. and Stryer, L. In *Biochemistry*; W. H. Freeman and Company, (2002).
[6] Sosa Torres, M. E., Saucedo-Vázquez, J. P. and Kroneck, P. M. H. In *Sustaining Life on Planet Earth: Metalloenzymes Mastering Dioxygen and Other Chewy Gases*; Kroneck, P. M. H., Sosa Torres, M. E., Eds.; Metal Ions in Life Sciences; Springer International Publishing: Switzerland, (2015); Vol. 15, pp. 1–12.
[7] Teichert, J. S., Kruse, F. M. and Trapp, O. (2019) Angew. Chem. Int. Ed., 58, 9944–9947.
[8] Grant, A., Lee, D. and Orengo, C. (2004) Genome Biol., 5, 1–9.
[9] Grigoryan, G. and DeGrado, W. F. (2011) J. Mol. Biol., 405, 1079–1100.
[10] Kolodny, R., Pereyaslavets, L., Samson, A. O. and Levitt, M. (2013) Annu. Rev. Biophys., 42, 559–582.
[11] Zhang, J. and Grigoryan, G. In *Methods in Enzymology*; Elsevier, (2013); Vol. 523, pp. 21–40.

[12] Mackenzie, C. O., Zhou, J. and Grigoryan, G. (2016) Proc. Natl. Acad. Sci., 113, E7438–E7447.
[13] Zhou, J. and Grigoryan, G. (2015) Protein Sci., 24, 508–524.
[14] Chapman, S. K., Daff, S. and Munro, A. W. In *Metal Sites in Proteins and Models: Iron Centres*; Hill, H. A. O., Sadler, P. J., Thomson, A. J., Eds.; Structure and Bonding; Springer: Berlin, Heidelberg, (1997); pp. 39–70.
[15] Batinic-Haberle, I., Tovmasyan, A. and Spasojevic, I. (2015) Redox Biol., 5, 43–65.
[16] Buchler, J.W In *The Porphyrins, Volume 1*; NY, USA, (1979); Vol. I, pp. 389–483.
[17] Dolphin, D., Traylor, T. G. and Xie, L. Y. (1997) Acc. Chem. Res., 30, 251–259.
[18] Lombardi, A., Nastri, F. and Pavone, V. (2001) Chem. Rev., 101, 3165–3190.
[19] Poulos, T. L. (2014) Chem. Rev., 114, 3919–3962.
[20] O. Senge, M., A. MacGowan, S. and M. O'Brien, J. (2015) Chem. Commun., 51, 17031–17063.
[21] Scheidt, W. R. and Lee, Y. J. In *Metal Complexes with Tetrapyrrole Ligands I*; Buchler, J. W., Ed.; Structure and Bonding; Springer: Berlin, Heidelberg, (1987); pp. 1–70.
[22] Forman, A., Renner, M. W., Fujita, E., Barkigia, K. M., Evans, M. C. W., Smith, K. M. and Fajer, J. (1989) Isr. J. Chem., 29, 57–64.
[23] Senge, M. O. (2006) Chem. Commun., 243–256.
[24] Toma, H. E. and Araki, K. (2000) Coord. Chem. Rev., 196, 307–329.
[25] Fukuzumi, S. (2006) Bull. Chem. Soc. Jpn., 79, 177–195.
[26] Battersby, A. R. (2000) Nat. Prod. Rep., 17, 507–526.
[27] Shelnutt, J. A., Song, X.-Z., Ma, J.-G., Jia, S.-L., Jentzen, W., Medforth, C. J. and Medforth, C. J. (1998) Chem. Soc. Rev., 27, 31–42.
[28] Senge, M. O., Ryan, A. A., Letchford, K. A., MacGowan, S. A. and Mielke, T. (2014) Symmetry, 6, 781–843.
[29] Gruber, K., Puffer, B. and Kräutler, B. (2011) Chem. Soc. Rev., 40, 4346–4363.
[30] Kräutler, B. (2005) Biochem. Soc. Trans., 33, 806–810.
[31] Ragsdale, S. W. In *The Metal-Driven Biogeochemistry of Gaseous Compounds in the Environment*; Kroneck, P. M. H., Torres, M. E. S., Eds.; Metal Ions in Life Sciences; Springer Netherlands: Dordrecht, (2014); pp. 125–145.
[32] Walker, F. A. and Simonis, U. In *Encyclopedia of Inorganic and Bioinorganic Chemistry*; American Cancer Society, (2011).
[33] Chino, M., Leone, L., Zambrano, G., Pirro, F., D'Alonzo, D., Firpo, V., Aref, D., Lista, L., Maglio, O., Nastri, F. and Lombardi, A. (2018) Biopolymers, 109, e23107.
[34] Baglia, R. A., Zaragoza, J. P. T. and Goldberg, D. P. (2017) Chem. Rev., 117, 13320–13352.
[35] Bren, K. L. (2016) Isr. J. Chem., 56, 693–704.
[36] Kleingardner, J. G. and Bren, K. L. (2015) Acc. Chem. Res., 48, 1845–1852.
[37] Ortiz de Montellano, P. R. (1987) Acc. Chem. Res., 20, 289–294.
[38] Perutz, M. F., Fermi, G., Luisi, B., Shaanan, B. and Liddington, R. C. (1987) Acc. Chem. Res., 20, 309–321.
[39] Perutz, M. F., Wilkinson, A. J., Paoli, M. and Dodson, G. G. (1998) Annu. Rev. Biophys. Biomol. Struct., 27, 1–34.
[40] Yamada, K., Ishikawa, H., Mizuno, M., Shibayama, N. and Mizutani, Y. (2013) J. Phys. Chem. B, 117, 12461–12468.
[41] Frauenfelder, H., McMahon, B. H. and Fenimore, P. W. (2003) Proc. Natl. Acad. Sci. U. S. A., 100, 8615–8617.
[42] Huang, X. and Groves, J. T. (2018) Chem. Rev., 118, 2491–2553.

[43] Ikeda-Saito, M. and Raven, E. *Dioxygen-dependent Heme Enzymes*; Metallobiology; RSC books, (2018).
[44] Wikström, M., Krab, K. and Sharma, V. (2018) Chem. Rev., 118, 2469–2490.
[45] Raven, E. and Dunford, B. *Heme Peroxidases*; Metallobiology; The Royal Society of Chemistry: Cambridge, (2016).
[46] Hofrichter, M., Kellner, H., Pecyna, M. J. and Ullrich, R. In *Monooxygenase, Peroxidase and Peroxygenase Properties and Mechanisms of Cytochrome P450*; Hrycay, E. G., Bandiera, S. M., Eds.; Advances in Experimental Medicine and Biology; Springer International Publishing: Switzerland, (2015); Vol. 851, pp. 341–368.
[47] Hofrichter, M., Kellner, H., Herzog, R., Karich, A., Liers, C., Scheibner, K., Kimani, V. W. and Ullrich, R. In *Grand Challenges in Fungal Biotechnology*; Nevalainen, H., Ed.; Grand Challenges in Biology and Biotechnology; Springer International Publishing: Switzerland, (2020); pp. 369–403.
[48] Raven, E. L. (2017) J. Biol. Inorg. Chem., 22, 175–183.
[49] Ortiz de Montellano, P. R. *Cytochrome P450: Structure, Mechanism, and Biochemistry*; 4th ed.; Springer International Publishing: Switzerland, (2015); Vol. 1.
[50] Sono, M., Roach, M. P., Coulter, E. D. and Dawson, J. H. (1996) Chem. Rev., 96, 2841–2888.
[51] Chmièlnicka, J., Ohlsson, P.-I., Paul, K.-G. and Stigbrand, T. (1971) FEBS Lett., 17, 181–184.
[52] Raven, E. L. (2003) Nat. Prod. Rep., 20, 367–381.
[53] Gajhede, M. (2001) Biochem. Soc. Trans., 29, 91–99.
[54] Krest, C. M., Onderko, E. L., Yosca, T. H., Calixto, J. C., Karp, R. F., Livada, J., Rittle, J. and Green, M. T. (2013) J. Biol. Chem., 288, 17074–17081.
[55] Moody, P. C. E. and Raven, E. L. (2018) Acc. Chem. Res., 51, 427–435.
[56] Feducia, J., Dumarieh, R., Gilvey, L. B. G., Smirnova, T., Franzen, S. and Ghiladi, R. A. (2009) Biochemistry, 48, 995–1005.
[57] Alfonso-Prieto, M., Biarnés, X., Vidossich, P. and Rovira, C. (2009) J. Am. Chem. Soc., 131, 11751–11761.
[58] Domínguez, L., Sosa-Peinado, A. and Hansberg, W. (2010) Arch. Biochem. Biophys., 500, 82–91.
[59] Groves, J. T. (2014) Nat. Chem., 6, 89–91.
[60] Chino, M., Leone, L., Maglio, O., D'Alonzo, D., Pirro, F., Pavone, V., Nastri, F. and Lombardi, A. (2017) Angew. Chem. Int. Ed., 56, 15580–15583.
[61] Ortiz de Montellano, P. R. (2010) Chem. Rev., 110, 932–948.
[62] Meunier, B., de Visser, S. P. and Shaik, S. (2004) Chem. Rev., 104, 3947–3980.
[63] Guengerich, F. P. (2018) ACS Catal., 8, 10964–10976.
[64] Groves, J. T. and Van der Puy, M. (1976) J. Am. Chem. Soc., 98, 5290–5297.
[65] Huang, X. and Groves, J. T. (2017) J. Biol. Inorg. Chem. JBIC, 22, 185–207.
[66] Yosca, T. H., Rittle, J., Krest, C. M., Onderko, E. L., Silakov, A., Calixto, J. C., Behan, R. K. and Green, M. T. (2013) Science, 342, 825–829.
[67] Millett, E. S., Efimov, I., Basran, J., Handa, S., Mowat, C. G. and Raven, E. L. (2012) Curr. Opin. Chem. Biol., 16, 60–66.
[68] Chauhan, N., Thackray, S. J., Rafice, S. A., Eaton, G., Lee, M., Efimov, I., Basran, J., Jenkins, P. R., Mowat, C. G., Chapman, S. K. and Raven, E. L. (2009) J. Am. Chem. Soc., 131, 4186–4187.
[69] Efimov, I., Basran, J., Thackray, S. J., Handa, S., Mowat, C. G. and Raven, E. L. (2011) Biochemistry, 50, 2717–2724.

[70] Hino, T., Nagano, S., Sugimoto, H., Tosha, T. and Shiro, Y. (2012) Biochim. Biophys. Acta, 1817, 680–687.
[71] Ferguson-Miller, S. and Babcock, G. T. (1996) Chem. Rev., 96, 2889–2908.
[72] Brändén, G., Gennis, R. B. and Brzezinski, P. (2006) Biochim. Biophys. Acta BBA - Bioenerg., 1757, 1052–1063.
[73] van der Oost, J., de Boer, A. P., de Gier, J. W., Zumft, W. G., Stouthamer, A. H. and van Spanning, R. J. (1994) FEMS Microbiol. Lett., 121, 1–9.
[74] Maréchal, A., Xu, J.-Y., Genko, N., Hartley, A. M., Haraux, F., Meunier, B. and Rich, P. R. (2020) Proc. Natl. Acad. Sci. U. S. A., 117, 9349–9355.
[75] Sharma, V., Jambrina, P. G., Kaukonen, M., Rosta, E. and Rich, P. R. (2017) Proc. Natl. Acad. Sci. U. S. A., 114, E10339–E10348.
[76] Shimada, A., Hatano, K., Tadehara, H., Yano, N., Shinzawa-Itoh, K., Yamashita, E., Muramoto, K., Tsukihara, T. and Yoshikawa, S. (2018) J. Biol. Chem., 293, 14868–14879.
[77] Tosha, T. and Shiro, Y. (2013) IUBMB Life, 65, 217–226.
[78] Mahinthichaichan, P., Gennis, R. B. and Tajkhorshid, E. (2018) Biochim. Biophys. Acta Bioenerg., 1859, 712–724.
[79] Ishigami, I., Lewis-Ballester, A., Echelmeier, A., Brehm, G., Zatsepin, N. A., Grant, T. D., Coe, J. D., Lisova, S., Nelson, G., Zhang, S., Dobson, Z. F., Boutet, S., Sierra, R. G., Batyuk, A., Fromme, P., Fromme, R., Spence, J. C. H., Ros, A., Yeh, S.-R. and Rousseau, D. L. (2019) Proc. Natl. Acad. Sci. U. S. A., 116, 3572–3577.
[80] Brzezinski, P. and Gennis, R. B. (2008) J. Bioenerg. Biomembr., 40, 521–531.
[81] Blomberg, M. R. A. and Siegbahn, P. E. M. (2013) Biochim. Biophys. Acta, 1827, 826–833.
[82] Malkamäki, A., Meunier, B., Reidelbach, M., Rich, P. R. and Sharma, V. (2019) Biochim. Biophys. Acta Bioenerg., 1860, 717–723.
[83] Bhagi-Damodaran, A., Michael, M. A., Zhu, Q., Reed, J., Sandoval, B. A., Mirts, E. N., Chakraborty, S., Moënne-Loccoz, P., Zhang, Y. and Lu, Y. (2017) Nat. Chem., 9, 257–263.
[84] Lee, H. J., Reimann, J., Huang, Y. and Adelroth, P. (2012) Biochim. Biophys. Acta, 1817, 537–544.
[85] Hino, T., Matsumoto, Y., Nagano, S., Sugimoto, H., Fukumori, Y., Murata, T., Iwata, S. and Shiro, Y. (2010) Science, 330, 1666–1670.
[86] Pinakoulaki, E., Pfitzner, U., Ludwig, B. and Varotsis, C. (2002) J. Biol. Chem., 277, 13563–13568.
[87] Schiffer, A., Parey, K., Warkentin, E., Diederichs, K., Huber, H., Stetter, K. O., Kroneck, P. M. H. and Ermler, U. (2008) J. Mol. Biol., 379, 1063–1074.
[88] Lukat, P., Rudolf, M., Stach, P., Messerschmidt, A., Kroneck, P. M. H., Simon, J. and Einsle, O. (2008) Biochemistry, 47, 2080–2086.
[89] Parey, K., Warkentin, E., Kroneck, P. M. H. and Ermler, U. (2010) Biochemistry, 49, 8912–8921.
[90] Brânzanic, A. M. V., Ryde, U. and Silaghi-Dumitrescu, R. (2019) Chem. Commun. Camb. Engl., 55, 14047–14049.
[91] Baker, S. C., Saunders, N. F., Willis, A. C., Ferguson, S. J., Hajdu, J. and Fülöp, V. (1997) J. Mol. Biol., 269, 440–455.
[92] Hiroto, S., Miyake, Y. and Shinokubo, H. (2017) Chem. Rev., 117, 2910–3043.
[93] Diéguez, M., Bäckvall, J.-E. and Pàmies, O. *Artificial Metalloenzymes and MetalloDNAzymes in Catalysis: From Design to Applications*; WILEY-VCH Verlag GmbH & Co. KGaA: Weinheim, Germany, (2018).

[94] Bos, J. and Roelfes, G. (2014) Curr. Opin. Chem. Biol., 19, 135–143.
[95] Schwizer, F., Okamoto, Y., Heinisch, T., Gu, Y., Pellizzoni, M. M., Lebrun, V., Reuter, R., Köhler, V., Lewis, J. C. and Ward, T. R. (2018) Chem. Rev., 118, 142–231.
[96] Mirts, E. N., Bhagi-Damodaran, A. and Lu, Y. (2019) Acc. Chem. Res., 52, 935–944.
[97] Oohora, K., Onoda, A. and Hayashi, T. (2019) Acc. Chem. Res., 52, 945–954.
[98] Koebke, K. J. and Pecoraro, V. L. (2019) Acc. Chem. Res., 52, 1160–1167.
[99] Grayson, K. J. and Anderson, J. R. (2018) Curr. Opin. Struct. Biol., 51, 149–155.
[100] Baker, E. G., Bartlett, G. J., Porter Goff, K. L. and Woolfson, D. N. (2017) Acc. Chem. Res., 50, 2085–2092.
[101] Lombardi, A., Pirro, F., Maglio, O., Chino, M. and DeGrado, W. F. (2019) Acc. Chem. Res., 52, 1148–1159.
[102] Churchfield, L. A. and Tezcan, F. A. (2019) Acc. Chem. Res., 52, 345–355.
[103] Natoli, S. N. and Hartwig, J. F. (2019) Acc. Chem. Res., 52, 326–335.
[104] Nastri, F., D'Alonzo, D., Leone, L., Zambrano, G., Pavone, V. and Lombardi, A. (2019) Trends Biochem. Sci., 44, 1022–1040.
[105] Peacock, A. F. A. (2016) Curr. Opin. Chem. Biol., 31, 160–165.
[106] Arnold, F. H. (2018) Angew. Chem. Int. Ed., 57, 4143–4148.
[107] Renata, H., Wang, Z. J. and Arnold, F. H. (2015) Angew. Chem. Int. Ed Engl., 54, 3351–3367.
[108] Oohora, K., Kihira, Y., Mizohata, E., Inoue, T. and Hayashi, T. (2013) J. Am. Chem. Soc., 135, 17282–17285.
[109] Oohora, K., Meichin, H., Kihira, Y., Sugimoto, H., Shiro, Y. and Hayashi, T. (2017) J. Am. Chem. Soc., 139, 18460–18463.
[110] Pott, M., Hayashi, T., Mori, T., Mittl, P. R. E., Green, A. P. and Hilvert, D. (2018) J. Am. Chem. Soc., 140, 1535–1543.
[111] Xu, J., Shoji, O., Fujishiro, T., Ohki, T., Ueno, T. and Watanabe, Y. (2012) Catal. Sci. Technol., 2, 739–744.
[112] Li, L.-L., Yuan, H., Liao, F., He, B., Gao, S.-Q., Wen, G.-B., Tan, X. and Lin, Y.-W. (2017) Dalton Trans., 46, 11230–11238.
[113] Liao, F., He, B., Du, K.-J., Gao, S.-Q., Wen, G.-B. and Lin, Y.-W. (2016) Chem. Lett., 45, 1087–1089.
[114] Liu, C., Yuan, H., Liao, F., Wei, C.-W., Du, K.-J., Gao, S.-Q., Tan, X. and Lin, Y.-W. (2019) Chem. Commun., 55, 6610–6613.
[115] Key, H. M., Dydio, P., Clark, D. S. and Hartwig, J. F. (2016) Nature, 534, 534–537.
[116] Oohora, K., Meichin, H., Zhao, L., Wolf, M. W., Nakayama, A., Hasegawa, J., Lehnert, N. and Hayashi, T. (2017) J. Am. Chem. Soc., 139, 17265–17268.
[117] Hayashi, T., Tinzl, M., Mori, T., Krengel, U., Proppe, J., Soetbeer, J., Klose, D., Jeschke, G., Reiher, M. and Hilvert, D. (2018) Nat. Catal., 1, 578–584.
[118] Sreenilayam, G. and Fasan, R. (2015) Chem. Commun., 51, 1532–1534.
[119] Tyagi, V., Bonn, R. B. and Fasan, R. (2015) Chem. Sci., 6, 2488–2494.
[120] Bordeaux, M., Tyagi, V. and Fasan, R. (2015) Angew. Chem., 127, 1764–1768.
[121] Sreenilayam, G., Moore, E. J., Steck, V. and Fasan, R. (2017) Adv. Synth. Catal., 359, 2076–2089.
[122] Sreenilayam, G., Moore, E. J., Steck, V. and Fasan, R. (2017) ACS Catal., 7, 7629–7633.
[123] Bhagi-Damodaran, A., Petrik, I. D., Marshall, N. M., Robinson, H. and Lu, Y. (2014) J. Am. Chem. Soc., 136, 11882–11885.
[124] Yu, Y., Mukherjee, A., Nilges, M. J., Hosseinzadeh, P., Miner, K. D. and Lu, Y. (2014) J. Am. Chem. Soc., 136, 1174–1177.

[125] Yeung, N., Lin, Y.-W., Gao, Y.-G., Zhao, X., Russell, B. S., Lei, L., Miner, K. D., Robinson, H. and Lu, Y. (2009) Nature, 462, 1079–1082.
[126] Bhagi-Damodaran, A., Reed, J. H., Zhu, Q., Shi, Y., Hosseinzadeh, P., Sandoval, B. A., Harnden, K. A., Wang, S., Sponholtz, M. R., Mirts, E. N., Dwaraknath, S., Zhang, Y., Moënne-Loccoz, P. and Lu, Y. (2018) Proc. Natl. Acad. Sci., 115, 6195–6200.
[127] Mukherjee, S., Mukherjee, M., Mukherjee, A., Bhagi-Damodaran, A., Lu, Y. and Dey, A. (2018) ACS Catal., 8, 8915–8924.
[128] Lin, Y.-W. (2017) Inorg. Chem. Front., 4, 918–920.
[129] Mirts, E. N., Petrik, I. D., Hosseinzadeh, P., Nilges, M. J. and Lu, Y. (2018) Science, 361, 1098–1101.
[130] Sadeghi, S. J., Tsotsou, G. E., Fairhead, M., Meharenna, Y. T. and Gilardi, G. In *Physics and Chemistry Basis of Biotechnology*; De Cuyper, M., Bulte, J. W. M., Eds.; Focus on Biotechnology; Springer Netherlands: Dordrecht, (2000); pp. 71–104.
[131] Fasan, R. (2012) ACS Catal., 2, 647–666.
[132] Di Nardo, G. and Gilardi, G. (2012) Int. J. Mol. Sci., 13, 15901–15924.
[133] Butler, C. F., Peet, C., Mason, A. E., Voice, M. W., Leys, D. and Munro, A. W. (2013) J. Biol. Chem., 288, 25387–25399.
[134] Shoji, O., Aiba, Y. and Watanabe, Y. (2019) Acc. Chem. Res., 52, 925–934.
[135] Ma, N., Chen, Z., Chen, J., Chen, J., Wang, C., Zhou, H., Yao, L., Shoji, O., Watanabe, Y. and Cong, Z. (2018) Angew. Chem. Int. Ed Engl., 57, 7628–7633.
[136] Shoji, O. and Watanabe, Y. (2014) JBIC J. Biol. Inorg. Chem., 19, 529–539.
[137] Kawakami, N., Shoji, O. and Watanabe, Y. (2011) Angew. Chem. Int. Ed., 50, 5315–5318.
[138] Shoji, O., Kunimatsu, T., Kawakami, N. and Watanabe, Y. (2013) Angew. Chem. Int. Ed., 52, 6606–6610.
[139] Karasawa, M., Stanfield, J. K., Yanagisawa, S., Shoji, O. and Watanabe, Y. (2018) Angew. Chem. Int. Ed., 57, 12264–12269.
[140] Coelho, P. S., Brustad, E. M., Kannan, A. and Arnold, F. H. (2013) Science, 339, 307–310.
[141] Coelho, P. S., Wang, Z. J., Ener, M. E., Baril, S. A., Kannan, A., Arnold, F. H. and Brustad, E. M. (2013) Nat. Chem. Biol., 9, 485–487.
[142] Farwell, C. C., Zhang, R. K., McIntosh, J. A., Hyster, T. K. and Arnold, F. H. (2015) ACS Cent. Sci., 1, 89–93.
[143] McIntosh, J. A., Coelho, P. S., Farwell, C. C., Wang, Z. J., Lewis, J. C., Brown, T. R. and Arnold, F. H. (2013) Angew. Chem. Int. Ed., 52, 9309–9312.
[144] Zhang, R. K., Chen, K., Huang, X., Wohlschlager, L., Renata, H. and Arnold, F. H. (2019) Nature, 565, 67–72.
[145] Brandenberg, O. F., Chen, K. and Arnold, F. H. (2019) J. Am. Chem. Soc., 141, 8989–8995.
[146] Wang, Z. J., Peck, N. E., Renata, H. and Arnold, F. H. (2014) Chem. Sci., 5, 598–601.
[147] Kan, S. B. J., Huang, X., Gumulya, Y., Chen, K. and Arnold, F. H. (2017) Nature, 552, 132–136.
[148] Kan, S. B. J., Lewis, R. D., Chen, K. and Arnold, F. H. (2016) Science, 354, 1048–1051.
[149] Brandenberg, O. F., Fasan, R. and Arnold, F. H. (2017) Curr. Opin. Biotechnol., 47, 102–111.
[150] Acevedo-Rocha, C. G., Gamble, C. G., Lonsdale, R., Li, A., Nett, N., Hoebenreich, S., Lingnau, J. B., Wirtz, C., Fares, C., Hinrichs, H., Deege, A., Mulholland, A. J., Nov, Y., Leys, D., McLean, K. J., Munro, A. W. and Reetz, M. T. (2018) ACS Catal., 8, 3395–3410.

[151] Sideri, A., Goyal, A., Di Nardo, G., Tsotsou, G. E. and Gilardi, G. (2013) J. Inorg. Biochem., 120, 1–7.
[152] Hammer, S. C., Kubik, G., Watkins, E., Huang, S., Minges, H. and Arnold, F. H. (2017) Science, 358, 215–218.
[153] Rentmeister, A., Arnold, F. H. and Fasan, R. (2009) Nat. Chem. Biol., 5, 26–28.
[154] Dennig, A., Weingartner, A. M., Kardashliev, T., Müller, C. A., Tassano, E., Schürmann, M., Ruff, A. J. and Schwaneberg, U. (2017) Chem. Weinh. Bergstr. Ger., 23, 17981–17991.
[155] Loskot, S. A., Romney, D. K., Arnold, F. H. and Stoltz, B. M. (2017) J. Am. Chem. Soc., 139, 10196–10199.
[156] Kleingardner, E. C., Asher, W. B. and Bren, K. L. (2017) Biochemistry, 56, 143–148.
[157] Osman, A. M., Koerts, J., Boersma, M. G., Boeren, S., Veeger, C. and Rietjens, I. M. C. M. (1996) Eur. J. Biochem., 240, 232–238.
[158] Kadnikova, E. N. and Kostić, N. M. (2003) J. Org. Chem., 68, 2600–2608.
[159] Dallacosta, C., Monzani, E. and Casella, L. (2003) J. Biol. Inorg. Chem., 8, 770–776.
[160] Ricoux, R., Lukowska, E., Pezzotti, F. and Mahy, J.-P. (2004) Eur. J. Biochem., 271, 1277–1283.
[161] Ricoux, R., Allard, M., Dubuc, R., Dupont, C., Maréchal, J.-D. and Mahy, J.-P. (2009) Org. Biomol. Chem., 7, 3208–3211.
[162] Wang, Q., Yang, Q. and Su, B. (2015) Electrochimica Acta, 161, 290–296.
[163] Gkaniatsou, E., Serre, C., Mahy, J.-P., Steunou, N., Ricoux, R. and Sicard, C. (2019) J. Porphyr. Phthalocyanines, 23, 718–728.
[164] Kleingardner, J. G., Kandemir, B. and Bren, K. L. (2014) J. Am. Chem. Soc., 136, 4–7.
[165] Robles, V. M., Maréchal, J.-D., Bahloul, A., Sari, M.-A., Mahy, J.-P. and Golinelli-Pimpaneau, B. (2012) PLoS ONE, 7, e51128.
[166] Mahammed, A., Gray, H. B., Weaver, J. J., Sorasaenee, K. and Gross, Z. (2004) Bioconjug. Chem., 15, 738–746.
[167] Mahammed, A. and Gross, Z. (2005) J. Am. Chem. Soc., 127, 2883–2887.
[168] Ricoux, R., Dubuc, R., Dupont, C., Marechal, J.-D., Martin, A., Sellier, M. and Mahy, J.-P. (2008) Bioconjug. Chem., 19, 899–910.
[169] Allard, M., Dupont, C., Robles, V. M., Doucet, N., Lledós, A., Maréchal, J.-D., Urvoas, A., Mahy, J.-P. and Ricoux, R. (2012) ChemBioChem, 13, 240–251.
[170] Mahajan, M. and Bhattacharjya, S. (2014) ChemBioChem, 15, 1257–1262.
[171] Cordova, J. M., Noack, P. L., Hilcove, S. A., Lear, J. D. and Ghirlanda, G. (2007) J. Am. Chem. Soc., 129, 512–518.
[172] Shinde, S., Cordova, J. M., Woodrum, B. W. and Ghirlanda, G. (2012) JBIC J. Biol. Inorg. Chem., 17, 557–564.
[173] Dürrenberger, M. and Ward, T. R. (2014) Curr. Opin. Chem. Biol., 19, 99–106.
[174] Lu, Y., Yeung, N., Sieracki, N. and Marshall, N. M. (2009) Nature, 460, 855–862.
[175] Petrik, I. D., Liu, J. and Lu, Y. (2014) Curr. Opin. Chem. Biol., 19, 67–75.
[176] Roiban, G.-D. and Reetz, M. T. (2015) Chem. Commun., 51, 2208–2224.
[177] Baltzer, L., Nilsson, H. and Nilsson, J. (2001) Chem. Rev., 101, 3153–3164.
[178] Korendovych, I. V. and DeGrado, W. F. (2020) Q. Rev. Biophys., 53, e3.
[179] Chino, M., Leone, L., Maglio, O. and Lombardi, A. (2016) Methods Enzymol., 580, 471–499.
[180] MacDonald, J. T., Maksimiak, K., Sadowski, M. I. and Taylor, W. R. (2010) Proteins Struct. Funct. Bioinforma., 78, 1311–1325.

[181] Yu, F., Cangelosi, V. M., Zastrow, M. L., Tegoni, M., Plegaria, J. S., Tebo, A. G., Mocny, C. S., Ruckthong, L., Qayyum, H. and Pecoraro, V. L. (2014) Chem. Rev., 114, 3495–3578.
[182] Kaiser, F., Eisold, A. and Labudde, D. (2015) J. Comput. Biol., 22, 698–713.
[183] Sasaki, T. and Kaiser, E. T. (1989) J. Am. Chem. Soc., 111, 380–381.
[184] Kamtekar, S., Schiffer, J. M., Xiong, H., Babik, J. M. and Hecht, M. H. (1993) Science, 262, 1680–1685.
[185] Bradley, L. H., Thumfort, P. P. and Hecht, M. H. (2006) Methods Mol. Biol., 340, 53–69.
[186] Patel, S. C., Bradley, L. H., Jinadasa, S. P. and Hecht, M. H. (2009) Protein Sci., 18, 1388–1400.
[187] Das, A. and Hecht, M. H. (2007) J. Inorg. Biochem., 101, 1820–1826.
[188] Patel, S. C. and Hecht, M. H. (2012) Protein Eng. Des. Sel., 25, 445–452.
[189] Huang, P.-S., Boyken, S. E. and Baker, D. (2016) Nature, 537, 320–327.
[190] Nanda, V. and Koder, R. L. (2010) Nat. Chem., 2, 15–24.
[191] Desjarlais, J. R. and Handel, T. M. (1995) Protein Sci., 4, 2006–2018.
[192] Bryson, J. W., Desjarlais, J. R., Handel, T. M. and DeGrado, W. F. (1998) Protein Sci., 7, 1404–1414.
[193] Tripet, B., Wagschal, K., Lavigne, P., Mant, C. T. and Hodges, R. S. (2000) J. Mol. Biol., 300, 377–402.
[194] Robertson, D. E., Farid, R. S., Moser, C. C., Urbauer, J. L., Mulholland, S. E., Pidikiti, R., Lear, J. D., Wand, A. J., DeGrado, W. F. and Dutton, P. L. (1994) Nature, 368, 425–432.
[195] Choma, C. T., Lear, J. D., Nelson, M. J., Dutton, P. L., Robertson, D. E. and DeGrado, W. F. (1994) J. Am. Chem. Soc., 116, 856–865.
[196] Koder, R. L., Anderson, J. L. R., Solomon, L. A., Reddy, K. S., Moser, C. C. and Dutton, P. L. (2009) Nature, 458, 305–309.
[197] Farid, T. A., Kodali, G., Solomon, L. A., Lichtenstein, B. R., Sheehan, M. M., Fry, B. A., Bialas, C., Ennist, N. M., Siedlecki, J. A., Zhao, Z., Stetz, M. A., Valentine, K. G., Anderson, J. L. R., Wand, A. J., Discher, B. M., Moser, C. C. and Dutton, P. L. (2013) Nat. Chem. Biol., 9, 826–833.
[198] Anderson, J. L. R., Armstrong, C. T., Kodali, G., Lichtenstein, B. R., Watkins, D. W., Mancini, J. A., Boyle, A. L., Farid, T. A., Crump, M. P., Moser, C. C. and Dutton, P. L. (2014) Chem. Sci., 5, 507–514.
[199] Watkins, D. W., Jenkins, J. M. X., Grayson, K. J., Wood, N., Steventon, J. W., Le Vay, K. K., Goodwin, M. I., Mullen, A. S., Bailey, H. J., Crump, M. P., MacMillan, F., Mulholland, A. J., Cameron, G., Sessions, R. B., Mann, S. and Anderson, J. L. R. (2017) Nat. Commun., 8, 1–9.
[200] Stenner, R., Steventon, J. W., Seddon, A. and Anderson, J. L. R. (2020) Proc. Natl. Acad. Sci., 117, 1419–1428.
[201] Huang, S. S., Gibney, B. R., Stayrook, S. E., Dutton, P. L. and Lewis, M. (2003) J. Mol. Biol., 326, 1219–1225.
[202] Faiella, M., Maglio, O., Nastri, F., Lombardi, A., Lista, L., Hagen, W. R. and Pavone, V. (2012) Chem. – Eur. J., 18, 15960–15971.
[203] Bender, G. M., Lehmann, A., Zou, H., Cheng, H., Fry, H. C., Engel, D., Therien, M. J., Blasie, J. K., Roder, H., Saven, J. G. and DeGrado, W. F. (2007) J. Am. Chem. Soc., 129, 10732–10740.
[204] Fry, H. C., Lehmann, A., Saven, J. G., DeGrado, W. F. and Therien, M. J. (2010) J. Am. Chem. Soc., 132, 3997–4005.
[205] Korendovych, I. V., Senes, A., Kim, Y. H., Lear, J. D., Fry, H. C., Therien, M. J., Blasie, J. K., Walker, F. A. and DeGrado, W. F. (2010) J. Am. Chem. Soc., 132, 15516–15518.

[206] Zhang, Z., Huang, L., Shulmeister, V. M., Chi, Y.-I., Kim, K. K., Hung, L.-W., Crofts, A. R., Berry, E. A. and Kim, S.-H. (1998) Nature, 392, 677–684.
[207] Polizzi, N. F., Wu, Y., Lemmin, T., Maxwell, A. M., Zhang, S.-Q., Rawson, J., Beratan, D. N., Therien, M. J. and DeGrado, W. F. (2017) Nat. Chem., 9, 1157–1164.
[208] Durley, R. C. E. and Mathews, F. S. (1996) Acta Crystallogr. D Biol. Crystallogr., 52, 65–76.
[209] Falzone, C. J., Wang, Y., Vu, B. C., Scott, N. L., Bhattacharya, S. and Lecomte, J. T. J. (2001) Biochemistry, 40, 4879–4891.
[210] Richardson, J. S. and Richardson, D. C. (2002) Proc. Natl. Acad. Sci. U. S. A., 99, 2754–2759.
[211] Ouberai, M., Dolphin, G. T., Dumy, P. and Garcia, J. (2011) Chem. Sci., 2, 1293–1300.
[212] Rufo, C. M., Moroz, Y. S., Moroz, O. V., Stöhr, J., Smith, T. A., Hu, X., DeGrado, W. F. and Korendovych, I. V. (2014) Nat. Chem., 6, 303–309.
[213] Andersen, J. F. and Montfort, W. R. (2000) J. Biol. Chem., 275, 30496–30503.
[214] Krieg, S., Huché, F., Diederichs, K., Izadi-Pruneyre, N., Lecroisey, A., Wandersman, C., Delepelaire, P. and Welte, W. (2009) Proc. Natl. Acad. Sci. U. S. A., 106, 1045–1050.
[215] D'Souza, A., Mahajan, M. and Bhattacharjya, S. (2016) Chem. Sci., 7, 2563–2571.
[216] D'Souza, A., Wu, X., Yeow, E. K. L. and Bhattacharjya, S. (2017) Angew. Chem. Int. Ed., 56, 5904–5908.
[217] D'Souza, A., Torres, J. and Bhattacharjya, S. (2018) Commun. Chem., 1, 78.
[218] Nastri, F., Lombardi, A., Morelli, G., Maglio, O., D'Auria, G., Pedone, C. and Pavone, V. (1997) Chem. – Eur. J., 3, 340–349.
[219] Nastri, F., Lombardi, A., D'Andrea, L. D., Sanseverino, M., Maglio, O. and Pavone, V. (1998) Biopolymers, 47, 5–22.
[220] Cowley, A. B., Kennedy, M. L., Silchenko, S., Lukat-Rodgers, G. S., Rodgers, K. R. and Benson, D. R. (2006) Inorg. Chem., 45, 9985–10001.
[221] Arnold, P. A., Benson, D. R., Brink, D. J., Hendrich, M. P., Jas, G. S., Kennedy, M. L., Petasis, D. T. and Wang, M. (1997) Inorg. Chem., 36, 5306–5315.
[222] Kennedy, M. L., Silchenko, S., Houndonougbo, N., Gibney, B. R., Dutton, P. L., Rodgers, K. R. and Benson, D. R. (2001) J. Am. Chem. Soc., 123, 4635–4636.
[223] Huffman, D. L., Rosenblatt, M. M. and Suslick, K. S. (1998) J. Am. Chem. Soc., 120, 6183–6184.
[224] Sakamoto, S., Obataya, I., Ueno, A. and Mihara, H. (1999) Chem. Commun., 1111–1112.
[225] Williamson, D. A. and Benson, D. R. (1998) Chem. Commun., 961–962.
[226] Liu, D., Williamson, D. A., Kennedy, M. L., Williams, T. D., Morton, M. M. and Benson, D. R. (1999) J. Am. Chem. Soc., 121, 11798–11812.
[227] Rosenblatt, M. M., Huffman, D. L., Wang, X., Remmer, H. A. and Suslick, K. S. (2002) J. Am. Chem. Soc., 124, 12394–12395.
[228] Rosenblatt, M. M., Wang, J. and Suslick, K. S. (2003) Proc. Natl. Acad. Sci., 100, 13140–13145.
[229] Liu, D., Lee, K.-H. and Benson, D. R. (1999) Chem. Commun., 1205–1206.
[230] Lombardi, A., Marasco, D., Maglio, O., Di Costanzo, L., Nastri, F. and Pavone, V. (2000) Proc. Natl. Acad. Sci., 97, 11922–11927.
[231] Schechter, A. N. (2008) Blood, 112, 3927–3938.
[232] Goodsell, D. S. and Olson, A. J. (2000) Annu. Rev. Biophys. Biomol. Struct., 29, 105–153.
[233] O'Neil, K. T. and DeGrado, W. F. (1990) Science, 250, 646–651.
[234] Nastri, F., Lombardi, A., Morelli, G., Pedone, C., Pavone, V., Chottard, G., Battioni, P. and Mansuy, D. (1998) J. Biol. Inorg. Chem., 3, 671–681.

[235] D'Auria, G., Maglio, O., Nastri, F., Lombardi, A., Mazzeo, M., Morelli, G., Paolillo, L., Pedone, C. and Pavone, V. (1997) Chem. – Eur. J., 3, 350–362.
[236] Woody, R. W., Kiefl, C., Sreerama, N., Lu, Y., Qiu, Y. and Shelnutt, J. A. In *Insulin & Related Proteins - Structure to Function and Pharmacology*; Dieken, M. L., Federwisch, M., De Meyts, P., Eds.; Springer Netherlands: Dordrecht, (2002); pp. 233–248.
[237] Woody, R. W. and Pescitelli, G. (2014) Z. Für Naturforschung A, 69, 313–325.
[238] Aojula, H. S., Wilson, M. T., Moore, G. R. and Williamson, D. J. (1988) Biochem. J., 250, 853–858.
[239] Lombardi, A., Nastri, F., Sanseverino, M., Maglio, O., Pedone, C. and Pavone, V. (1998) Inorganica Chim. Acta, 275–276, 301–313.
[240] Doig, A. J. and Baldwin, R. L. (1995) Protein Sci., 4, 1325–1336.
[241] Chino, M., Maglio, O., Nastri, F., Pavone, V., DeGrado, W. F. and Lombardi, A. (2015) Eur. J. Inorg. Chem., 2015, 3371–3390.
[242] Summa, C. M., Rosenblatt, M. M., Hong, J.-K., Lear, J. D. and DeGrado, W. F. (2002) J. Mol. Biol., 321, 923–938.
[243] Lombardi, A., Nastri, F., Marasco, D., Maglio, O., Sanctis, G. D., Sinibaldi, F., Santucci, R., Coletta, M. and Pavone, V. (2003) Chem. – Eur. J., 9, 5643–5654.
[244] Di Costanzo, L., Geremia, S., Randaccio, L., Nastri, F., Maglio, O., Lombardi, A. and Pavone, V. (2004) J. Biol. Inorg. Chem., 9, 1017–1027.
[245] Vicari, C., Saraiva, I. H., Maglio, O., Nastri, F., Pavone, V., Louro, R. O. and Lombardi, A. (2014) Chem. Commun., 50, 3852–3855.
[246] Liu, J., Chakraborty, S., Hosseinzadeh, P., Yu, Y., Tian, S., Petrik, I., Bhagi, A. and Lu, Y. (2014) Chem. Rev., 114, 4366–4469.
[247] Del Gatto, G. Synthesis and structural characterization of artificial metalloproteins. PhD Thesis in Chemical Sciences, XX Cycle, University of Naples "Federico II," (2007).
[248] Ranieri, A., Monari, S., Sola, M., Borsari, M., Battistuzzi, G., Ringhieri, P., Nastri, F., Pavone, V. and Lombardi, A. (2010) Langmuir, 26, 17831–17835.
[249] Vitale, R., Lista, L., Lau-Truong, S., Tucker, R. T., Brett, M. J., Limoges, B., Pavone, V., Lombardi, A. and Balland, V. (2014) Chem. Commun., 50, 1894–1896.
[250] Nastri, F., Lista, L., Ringhieri, P., Vitale, R., Faiella, M., Andreozzi, C., Travascio, P., Maglio, O., Lombardi, A. and Pavone, V. (2011) Chem. – Eur. J., 17, 4444–4453.
[251] Zambrano, G., Ruggiero, E., Malafronte, A., Chino, M., Maglio, O., Pavone, V., Nastri, F. and Lombardi, A. (2018) Int. J. Mol. Sci., 19, 2896.
[252] Green, A. P., Hayashi, T., Mittl, P. R. E. and Hilvert, D. (2016) J. Am. Chem. Soc., 138, 11344–11352.
[253] Munro, O. Q., de Wet, M., Pollak, H., Wyk, J. van and Marques, H. M. (1998) J. Chem. Soc. Faraday Trans., 94, 1743–1752.
[254] Weiss, R., Gold, A. and Terner, J. (2006) Chem. Rev., 106, 2550–2579.
[255] Perrella, F., Raucci, U., Chiariello, M. G., Chino, M., Maglio, O., Lombardi, A. and Rega, N. (2018) Biopolymers, 109, e23225.
[256] Battistuzzi, G., Bellei, M., Zederbauer, M., Furtmüller, P. G., Sola, M. and Obinger, C. (2006) Biochemistry, 45, 12750–12755.
[257] Battistuzzi, G., Bellei, M., Vlasits, J., Banerjee, S., Furtmüller, P. G., Sola, M. and Obinger, C. (2010) Arch. Biochem. Biophys., 494, 72–77.
[258] Battistuzzi, G., Stampler, J., Bellei, M., Vlasits, J., Soudi, M., Furtmüller, P. G. and Obinger, C. (2011) Biochemistry, 50, 7987–7994.
[259] Battistuzzi, G., Bellei, M., Bortolotti, C. A. and Sola, M. (2010) Arch. Biochem. Biophys., 500, 21–36.

[260] Ayala, M., Roman, R. and Vazquez-Duhalt, R. (2007) Biochem. Biophys. Res. Commun., 357, 804–808.
[261] Abdel-Hamid, A. M., Solbiati, J. O. and Cann, I. K. O. In *Advances in Applied Microbiology*; Sariaslani, S., Gadd, G. M., Eds.; Academic Press, (2013); Vol. 82, pp. 1–28.
[262] Auriemma, F., De Rosa, C., Malafronte, A., Di Girolamo, R., Santillo, C., Gerelli, Y., Fragneto, G., Barker, R., Pavone, V., Maglio, O. and Lombardi, A. (2017) ACS Appl. Mater. Interfaces, 9, 29318–29327.
[263] Vitale, R., Lista, L., Cerrone, C., Caserta, G., Chino, M., Maglio, O., Nastri, F., Pavone, V. and Lombardi, A. (2015) Org. Biomol. Chem., 13, 4858–4868.
[264] Savenkova, M. I., Kuo, J. M. and Ortiz de Montellano, P. R. (1998) Biochemistry, 37, 10828–10836.
[265] Berglund, G. I., Carlsson, G. H., Smith, A. T., Szöke, H., Henriksen, A. and Hajdu, J. (2002) Nature, 417, 463–468.
[266] Caserta, G., Chino, M., Firpo, V., Zambrano, G., Leone, L., D'Alonzo, D., Nastri, F., Maglio, O., Pavone, V. and Lombardi, A. (2018) ChemBioChem, 19, 1823–1826.
[267] Oliva, R., Chino, M., Pane, K., Pistorio, V., De Santis, A., Pizzo, E., D'Errico, G., Pavone, V., Lombardi, A., Del Vecchio, P., Notomista, E., Nastri, F. and Petraccone, L. (2018) Sci. Rep., 8, 8888.
[268] Di Blasio, B., Pavone, V., Lombardi, A., Pedone, C. and Benedetti, E. (1993) Biopolymers, 33, 1037–1049.
[269] Karle, I. L. (2001) Pept. Sci., 60, 351–365.
[270] Asayama, S., Mori, T., Nagaoka, S. and Kawakami, H. (2003) J. Biomater. Sci. Polym. Ed., 14, 1169–1179.
[271] Asayama, S., Kawamura, E., Nagaoka, S. and Kawakami, H. (2006) Mol. Pharm., 3, 468–470.
[272] Batinic-Haberle, I., Tovmasyan, A. and Spasojevic, I. (2015) Redox Biol., 5, 43–65.
[273] Liu, W., Huang, X., Cheng, M.-J., Nielsen, R. J., Goddard, W. A. and Groves, J. T. (2012) Science, 337, 1322–1325.
[274] Liu, W. and Groves, J. T. (2013) Angew. Chem. Int. Ed., 52, 6024–6027.
[275] Li, G., Dilger, A. K., Cheng, P. T., Ewing, W. R. and Groves, J. T. (2018) Angew. Chem. Int. Ed Engl., 57, 1251–1255.
[276] Jin, N. and Groves, J. T. (1999) J. Am. Chem. Soc., 121, 2923–2924.
[277] Song, W. J., Seo, M. S., George, S. D., Ohta, T., Song, R., Kang, M.-J., Tosha, T., Kitagawa, T., Solomon, E. I. and Nam, W. (2007) J. Am. Chem. Soc., 129, 1268–1277.
[278] Guo, M., Dong, H., Li, J., Cheng, B., Huang, Y., Feng, Y. and Lei, A. (2012) Nat. Commun., 3, 1–9.
[279] Arunkumar, C., Lee, Y.-M., Lee, J. Y., Fukuzumi, S. and Nam, W. (2009) Chem. - Eur. J., 15, 11482–11489.
[280] Neu, H. M., Yang, T., Baglia, R. A., Yosca, T. H., Green, M. T., Quesne, M. G., de Visser, S. P. and Goldberg, D. P. (2014) J. Am. Chem. Soc., 136, 13845–13852.
[281] Taniguchi, I., Li, C., Ishida, M. and Yao, Q. (1999) J. Electroanal. Chem., 460, 245–250.
[282] Khan, K. K., Mondal, M. S. and Mitra, S. (1996) J. Chem. Soc. Dalton Trans., 0, 1059–1062.
[283] Khan, K. K., Mondal, M. S. and Mitra, S. (1998) J. Chem. Soc. Dalton Trans., 533–536.
[284] Cai, Y.-B., Li, X.-H., Jing, J. and Zhang, J.-L. (2013) Metallomics, 5, 828–835.
[285] Cai, Y.-B., Yao, S.-Y., Hu, M., Liu, X. and Zhang, J.-L. (2016) Inorg. Chem. Front., 3, 1236–1244.

[286] Leone, L., D'Alonzo, D., Balland, V., Zambrano, G., Chino, M., Nastri, F., Maglio, O., Pavone, V. and Lombardi, A. (2018) Front. Chem., 6.
[287] Primus, J.-L., Grunenwald, S., Hagedoorn, P.-L., Albrecht-Gary, A.-M., Mandon, D. and Veeger, C. (2002) J. Am. Chem. Soc., 124, 1214–1221.
[288] Colonna, S., Gaggero, N., Carrea, G. and Pasta, P. (1992) J. Chem. Soc. Chem. Commun., 1992, 357–358.
[289] Ohashi, M., Koshiyama, T., Ueno, T., Yanase, M., Fujii, H. and Watanabe, Y. (2003) Angew. Chem. Int. Ed., 42, 1005–1008.
[290] Garner, D. K., Liang, L., Barrios, D. A., Zhang, J.-L. and Lu, Y. (2011) ACS Catal., 1, 1083–1089.
[291] Sansiaume-Dagousset, E., Urvoas, A., Chelly, K., Ghattas, W., Maréchal, J.-D., Mahy, J.-P. and Ricoux, R. (2014) Dalton Trans., 43, 8344–8354.
[292] Tang, J., Huang, F., Wei, Y., Bian, H., Zhang, W. and Liang, H. (2016) Dalton Trans., 45, 8061–8072.
[293] Roger, I., Shipman, M. A. and Symes, M. D. (2017) Nat. Rev. Chem., 1, 1–13.
[294] Esswein, A. J. and Nocera, D. G. (2007) Chem. Rev., 107, 4022–4047.
[295] Caserta, G., Roy, S., Atta, M., Artero, V. and Fontecave, M. (2015) Curr. Opin. Chem. Biol., 25, 36–47.
[296] Artero, V. (2017) Nat. Energy, 2, 1–6.
[297] Le, J. M. and Bren, K. L. (2019) ACS Energy Lett., 4, 2168–2180.
[298] Onoda, A. and Hayashi, T. (2015) Curr. Opin. Chem. Biol., 25, 133–140.
[299] Lubitz, W., Ogata, H., Rüdiger, O. and Reijerse, E. (2014) Chem. Rev., 114, 4081–4148.
[300] Vincent, K. A., Parkin, A. and Armstrong, F. A. (2007) Chem. Rev., 107, 4366–4413.
[301] Stiebritz, M. T. and Reiher, M. (2012) Chem. Sci., 3, 1739–1751.
[302] Artero, V., Chavarot-Kerlidou, M. and Fontecave, M. (2011) Angew. Chem. Int. Ed., 50, 7238–7266.
[303] Dempsey, J. L., Brunschwig, B. S., Winkler, J. R. and Gray, H. B. (2009) Acc. Chem. Res., 42, 1995–2004.
[304] Eckenhoff, W. T., McNamara, W. R., Du, P. and Eisenberg, R. (2013) Biochim. Biophys. Acta, 1827, 958–973.
[305] Bacchi, M., Berggren, G., Niklas, J., Veinberg, E., Mara, M. W., Shelby, M. L., Poluektov, O. G., Chen, L. X., Tiede, D. M., Cavazza, C., Field, M. J., Fontecave, M. and Artero, V. (2014) Inorg. Chem., 53, 8071–8082.
[306] Kandemir, B., Kubie, L., Guo, Y., Sheldon, B. and Bren, K. L. (2016) Inorg. Chem., 55, 1355–1357.
[307] Call, A., Casadevall, C., Romero-Rivera, A., Martin-Diaconescu, V., Sommer, D. J., Osuna, S., Ghirlanda, G. and Lloret-Fillol, J. (2019) ACS Catal., 9, 5837–5846.
[308] Baffert, C., Artero, V. and Fontecave, M. (2007) Inorg. Chem., 46, 1817–1824.
[309] Lee, C. H., Dogutan, D. K. and Nocera, D. G. (2011) J. Am. Chem. Soc., 133, 8775–8777.
[310] McCrory, C. C. L., Uyeda, C. and Peters, J. C. (2012) J. Am. Chem. Soc., 134, 3164–3170.
[311] Sommer, D. J., Vaughn, M. D. and Ghirlanda, G. (2014) Chem. Commun., 50, 15852–15855.
[312] Sommer, D. J., Vaughn, M. D., Clark, B. C., Tomlin, J., Roy, A. and Ghirlanda, G. (2016) Biochim. Biophys. Acta BBA - Bioenerg., 1857, 598–603.
[313] Kandemir, B., Chakraborty, S., Guo, Y. and Bren, K. L. (2016) Inorg. Chem., 55, 467–477.
[314] Firpo, V., Le, J. M., Pavone, V., Lombardi, A. and Bren, K. L. (2018) Chem. Sci., 9, 8582–8589.

[315] Kundu, A. and Kishore, N. (2004) Biophys. Chem., 109, 427–442.
[316] Bediako, D. K., Solis, B. H., Dogutan, D. K., Roubelakis, M. M., Maher, A. G., Lee, C. H., Chambers, M. B., Hammes-Schiffer, S. and Nocera, D. G. (2014) Proc. Natl. Acad. Sci. U. S. A., 111, 15001–15006.
[317] Le, J. M., Alachouzos, G., Chino, M., Frontier, A. J., Lombardi, A. and Bren, K. L. (2020) Biochemistry, 59, 1289–1297.
[318] Costentin, C. and Savéant, J.-M. (2014) ChemElectroChem, 1, 1226–1236.
[319] Rountree, E. S., McCarthy, B. D., Eisenhart, T. T. and Dempsey, J. L. (2014) Inorg. Chem., 53, 9983–10002.

TABLES

Table 1. Characterization of Mimochrome IV analogues.

Compound	CD Soret sign	Soret band (ε)[a]	Q bands[a]	pKa_{His}	$E°'(Fe^{3+}/Fe^{2+})$ vs SHE (pH 7)[a]
Fe(III)-MC4	+	401 (103)	522;560	3.85	-80[b]; -85[c]
Fe(III)-MC4E	+	401 (96)	522;560	3.85	-169[c]
Fe(III)-MC4K	+	402 (101)	522;560	2.63	-20[c]
Fe(III)-MC6	+ ; – [d]	391 (63)	490;520_{sh};610	3.4	-99[e]; -106[e]; -111[f]

[a] Wavelengths are reported in nm; molar absorption coefficients in mM^{-1} cm^{-1}; redox potentials in mV.
[b] Taken from ref. [243]
[c] Taken from ref. [247]
[d] Positive to negative transition upon TFE addition
[e] In diffusion and adsorbed on hydrophobically-coated gold electrode, respectively. Taken from ref. [248]
[f] Adsorbed on ITO electrode. Taken from ref. [249]

Table 2. Comparison of the kinetic parameters for H_2O_2-dependent oxidation of ABTS catalyzed by mimochromes and HRP. Data from ref. [266].

		ABTS	H_2O_2		ABTS	H_2O_2	
Catalyst	**pH**	K_m (mM)	K_m (mM)	k_{cat} (s^{-1})	k_{cat}/K_m ($mM^{-1}s^{-1}$)	k_{cat}/K_m ($mM^{-1}s^{-1}$)	**TON**
FeMC6*a	6.5	9.0	4.4×10^2	5.8×10^3	6.4×10^4	1.3×10^1	14 000
FeMC6*	6.5	5.0	1.3×10^2	2.3×10^3	4.6×10^4	1.8×10^1	5 900
HRP	4.6	7.0×10^1	9.3×10^{-1}	2.8×10^3	3.8×10^3	2.9×10^3	50 000

1 **Table 3.** Enzyme-catalyzed H_2O_2-dependent oxidation of thioanisole.

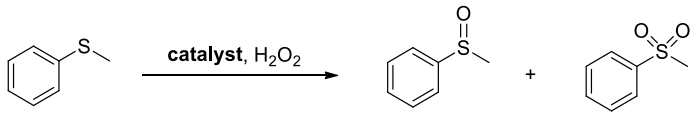

Catalyst	Catalyst:substrate:H_2O_2 (catalyst concentration)	Yield, % (time, min)	TON	Reference
MnMC6*a	1:100:100 (20 μM)	100 (5)	870[a]	[286]
FeMC6*a	1:100:100 (20 μM)	97 (5)	1500[b]	[286]
Mn-HRP	1:100:100 (9 μM)	4 (5)	4	[286]
Fe-HRP	1:30:40 (330 μM)	95 (60)	28	[288]
Cr-salophen-Mb(H64D/A71G)	1:100:100 (10 μM)	–[c]	–[c]	[289]
Mn-Cor-BSA	1:50:75 (200 μM)	83 (90)	150	[167]
Fe(T*p*CPP)-Xln10A	1:425:175 (20 μM)	85 (138)	145	[161]
Mn-salen-Mb(T39C/L72C)	1:40:40 (130 μM)	17 (10)	7[d]	[290]
Fe-T*p*SPP-NCS-3.24	1:500:500 (5 μM)	1.3 (120)	6.5[d]	[291]
CoL-BSA	1:100;150 (2.7 μM)	98 (1680)	98[d]	[292]

[a] TON was determined used a 1:1000:1000 catalyst:substrate:H_2O_2 ratio.

[b] TON was determined used a 1:2000:2000 catalyst:substrate:H_2O_2 ratio.

[c] Yield and TON are not available from the reference. The reported reaction rate is 78 10^{-3} TON min^{-1}.

[d] TON was calculated based on the reported yield and catalyst:substrate ratio.

2

FIGURE LEGENDS

Figure 1. Porphyrin modulation in Nature could be classified under the following design strategies, from the innermost to the outermost: metal ion selection (red), cofactor modification (blue), environment modulation (green).

Figure 2. Selected heme centers as found in natural proteins. Each protein is represented by its active site, with non-metal and metal atoms depicted as sticks and balls, respectively. The fifth axial ligand, also referred to as proximal, is depicted below the porphyrin plane. Native function is defined below each active site. (PDB IDs: bovine cytochrome b5, 1CYO; horse heart cytochrome c, 1AKK; recombinant sperm whale myoglobin, 2W6W; recombinant horseradish peroxidase C1a, 1ATJ; recombinant cytochrome P450cam, 5CP4; nitric oxide reductase from *Roseobacter denitrificans*, 4XYD; human cytochrome c oxidase, 5ZS2; sulfite reductase from *E. Coli*, 1AOP).

Figure 3. Reaction scheme for heme-catalysed dioxygen and hydrogen peroxide activation. The heme macrocycle is represented as a black circle. Protons and the protein-derived iron axial ligand are not shown for sake of simplicity. Sub, Sub-O and Sub-(O)2 denote the substrate, the mono-oxygenated and the doubly oxygenated product, respectively.

Figure 4. Mimochrome I design process through miniaturization. (A and B) Active-site was identified from Hb β chain (PDB ID: 2HHB) and extracted. (C) Heme-covering nonapeptide was isolated. (D) Wise rotamer selection allowed for a mutual approach of heme propionate towards Lys95. (E) Solvent exposed residues were redesigned and deuteroporphyrin IX was preferred over protoporphyrin IX for synthetic reasons. (F) Finally, C_2 symmetry operation led to the *hexa*-coordinated deuteroheme.

Scheme 1. Mimochrome peptide sequences. R and R' are either identical or different. Proximal and distal axial residues are indicated in bold.

Figure 5. Δ and Λ diastereomers of Co(III)-Mimochrome I. (A) NMR-derived average molecular structures. (B) Schematic representation of the two possible orientations of the peptide chains around the metal center, which give rise to Δ and Λ diastereomers. (C) Soret band CD spectra, which show a negative or a positive Cotton effect for the Δ and the Λ diastereomer, respectively.

Figure 6. Co(III)-Mimochrome IV NMR (A, PDB ID: 1VL3) and crystallographic (B, PDB ID: 1PYZ) models. Both structures show the Λ configuration around the metal ion, but a different

scheme of Glu1-Arg9 ion pairs. The designed *intra*-molecular *inter*-chain interactions were experimentally observed in solution, whereas *intra*-chain i←i+8 interactions were present in the solid state.

Figure 7. Designed models of *penta*-coordinated Mimochomes. (A) MC6; (B) MC6*; (C) MC6*a. The residues that have been mutated in each round of redesign are highlighted in magenta.

Figure 8. Fe(III)-Mimochrome peroxidase activity, freely diffusing and immobilized on AuNPs. (A,B) Progress curves for ABTS oxidation by H_2O_2, catalyzed by Fe(III)MC6 (solid line) and by corresponding monoadduct (dashed line), which misses the distal helical peptide, either in the presence (A) or in the absence (B) of 50 % TFE. (C) Progress curve in ABTS oxidation by H_2O_2, catalysed by Fe(III)-MC6Ser6Gly analogue. (D) Cartoon of Fe(III)-MC6Ser6Gly immobilized on AuNPs, through lipoic acid linkers. Readapted with permission of Wiley [250] and MDPI [251].

Figure 9. (A) Cartoon of MC6 and MC6*, highlighting the possible role of Arg10(*D*) in catalysis, when unable to make an *inter*-chain ion pair, upon Glu2Leu(*TD*) mutation. (B) Compound I stabilization, as observed in HRP crystal structure (PDB ID: 1HCH), highlighting the H-bond between Arg38 and the putative ferryl-oxygen, fundamental for peroxide heterolytic cleavage [265].

Figure 10. UV-Vis absorption spectra of (A) Mn- and (B) Fe-MC6*a in their resting (solid lines) and high-valent (dashed lines) states.

Figure 11. Cyclic voltamograms of (A) CoMC6*a and (B) CoMP11 acquired at different TFE concentrations. Adapted from ref. [314] with the permission of the American Chemical Society.